This work has been carried out within the framework of the EUROfusion Consortium and has received funding from the Euratom research and training programe 2014-2018 under grant agreement No 633053. The views and opinions expressed herein do not necessarily reflect those of the European Commission.

Recent progress towards a quantitative description of filamentary SOL transport

D. Carralero[1], M. Komm[2], M. Siccinio[1], S. A. Artene[1,3], F. D'Isa[1], J. Adamek[2], L. Aho-Mantila[4], G. Birkenmeier[1,3], M. Brix[5], G. Fuchert[1,6], M. Groth[7], T. Lunt[1], P. Manz[1,3], J. Madsen[8], S. Marsen[5,6], H. W. Müller[1,9], B. Sieglin[1], U. Stroth[1], H. J. Sun[1], N. Vianello[10,11], M. Wischmeier[1], E. Wolfrum[1], ASDEX Upgrade Team[1], COMPASS Team[2], JET Contributors[12] and the EUROfusion MST team[13].

[1]Max-Planck-Institut für Plasmaphysik, Garching, Germany. [2]Institute of Plasma Physics AS CR, Prague, Czech Republic. [3]Physik-Department E28, Technische Universität München, Garching, Germany. [4]VTT Technical Research Center of Finland, Helsinki, Finland. [5]EUROfusion Consortium, JET, Culham Science Centre, Abingdon,OX14 3DB, UK, [6]Max-Planck-Institut für Plasmaphysik, Greifswald, Germany. [7]Aalto University, Espoo, Finland. [8]The Technical University of Denmark, Department of Physics, DK-2800 Kgs. Lyngby, Denmark, [9]Institute of Materials Chemistry and Research, University of Vienna, Währingerstrasse 42, A-1090 Vienna, Austria. [10]Consorzio RFX, Associazione Euratom-ENEA sulla fusione, C.so Stati Uniti 4,I-35127 Padova, Italy. [11]Ecole Polytechnique Fédérale de Lausanne, Centre de Recherches en Physique des Plasmas, Lausanne, Switzerland. [12]See the author list of "Overview of the JET results in support to ITER" by X. Litaudon et al. to be published in Nuclear Fusion Special issue: overview and summary reports from the 26th Fusion Energy Conference (Kyoto, Japan, 17-22 October) [13]See http://www.euro-fusionscipub.org/mst1

26th International Atomic Energy Agency Fusion Energy Conference, Kyoto, Japan
October 19th, 2016

Wetted area ITER : <1m^2
Total surfaces : 680 m^2

Inter-ELM, attached power deposition profile

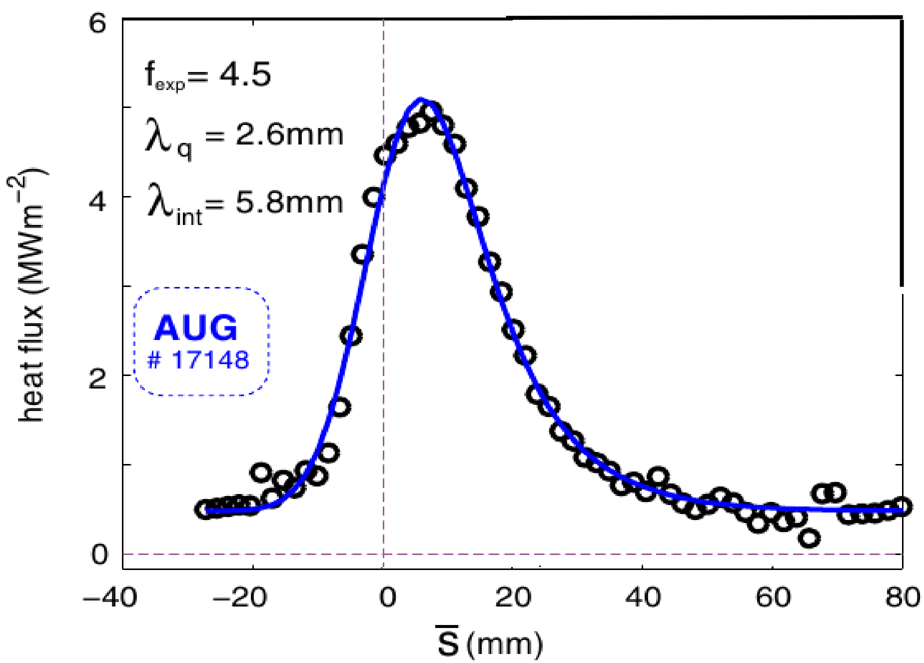

*T.Eich et al. PRL **107**, (2011)*

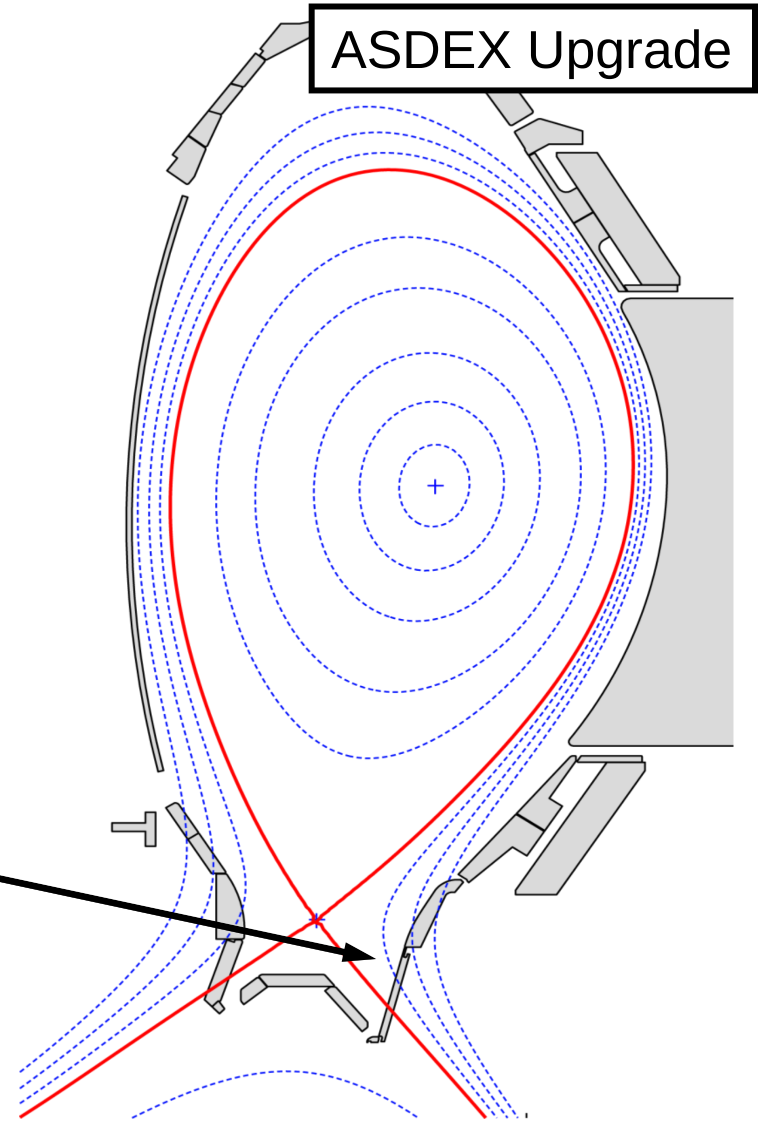

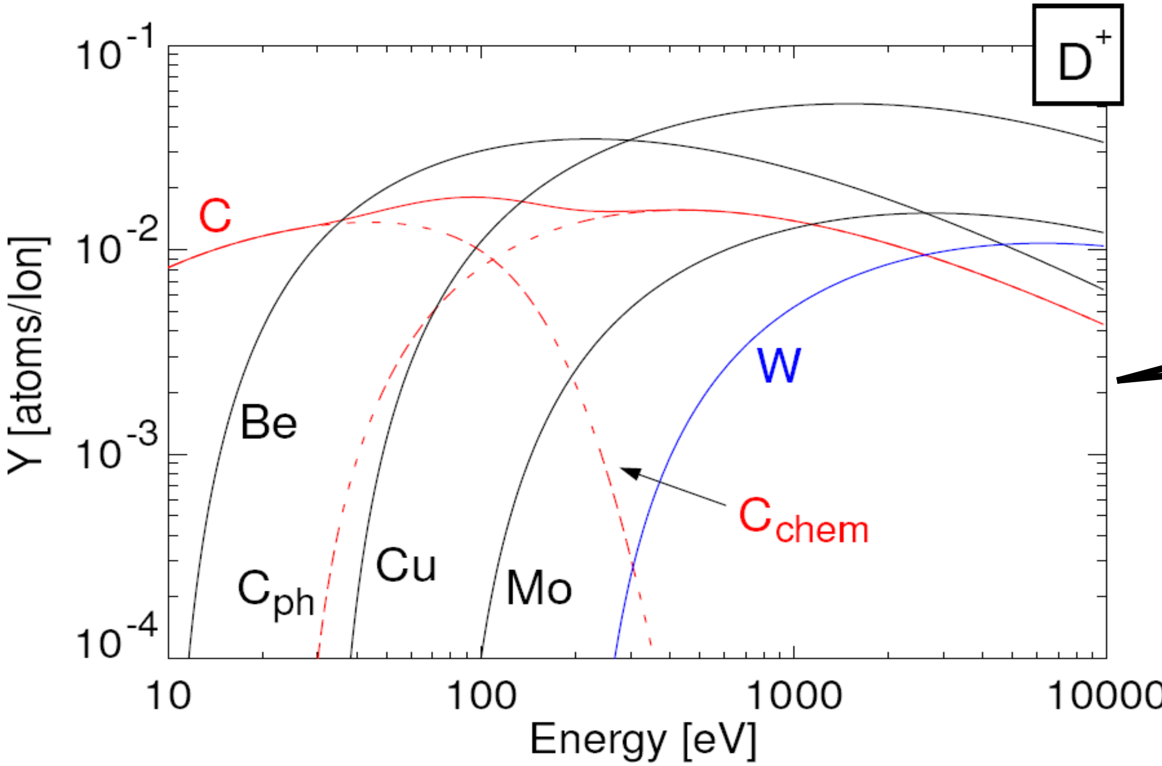

R.Dux, Habilitation (2004)

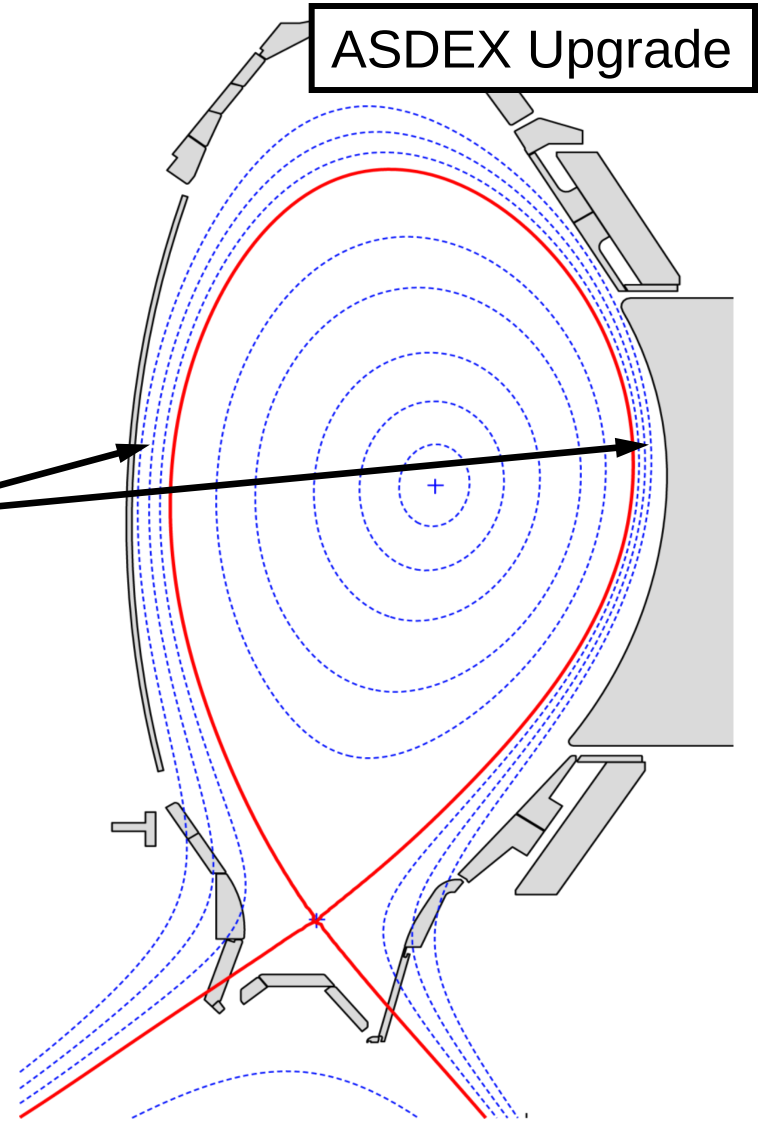

The Problem of Exhaust: $\Gamma_{||}$ vs. $\Gamma_{\perp}$

A key question for ITER & DEMO:

How are heat and particle fluxes distributed over the various plasma facing components?

In the SOL of a tokamak, this is strongly affected by the competition between **parallel conduction** and **perpendicular convection**.

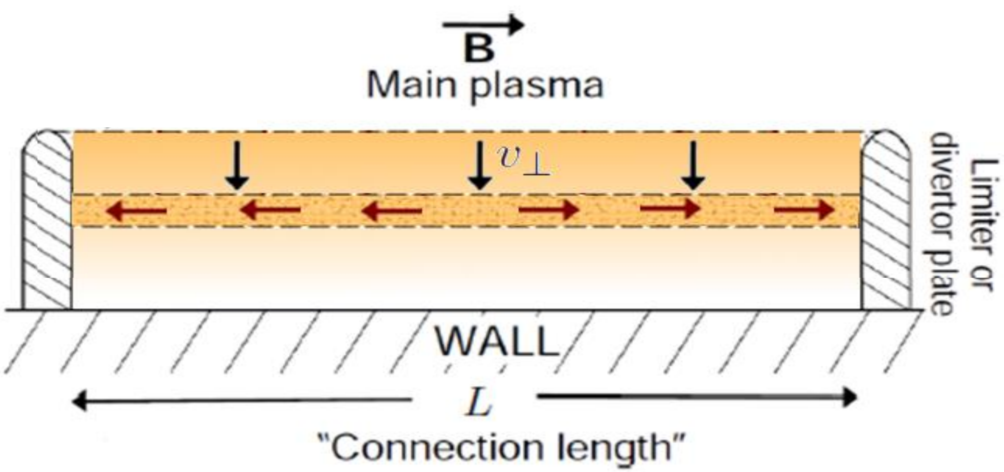

$$\tau_{||} = L/c_s$$

$$\lambda_{SOL} = \frac{v_\perp L}{c_s}$$

Shoulder formation

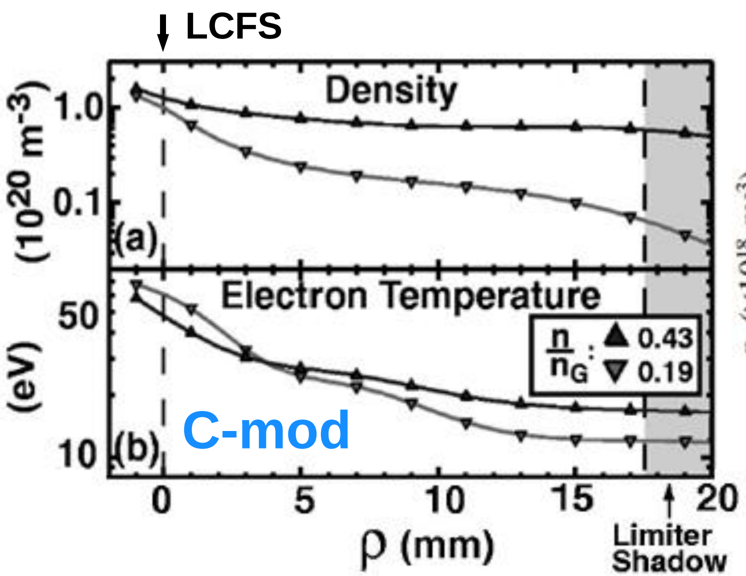

B. LaBombard, PoP , (2001)

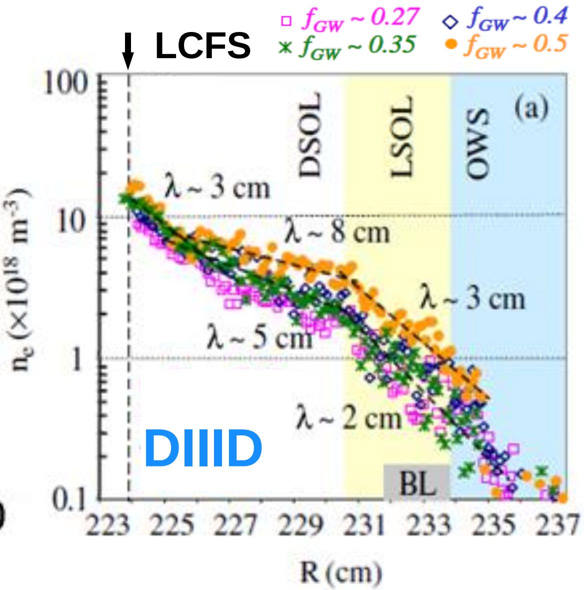

D.L. Rudakov, NF, (2005)

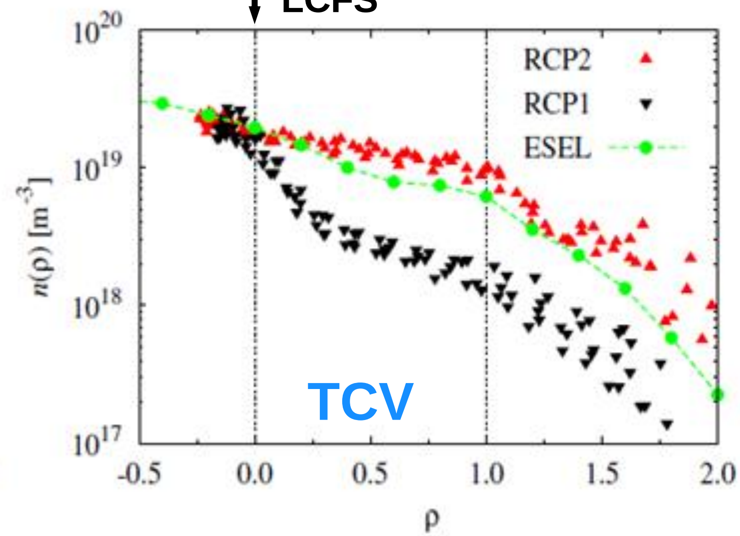

O. E. Garcia et al, JNM, (2007)

A well known experimental fact in tokamaks:

In L-mode, SOL density profiles flatten over a certain density threshold.

An increase of Γ_r associated to a **filament transition** has been proposed as the explanation in the literature.

Filaments and Shoulder

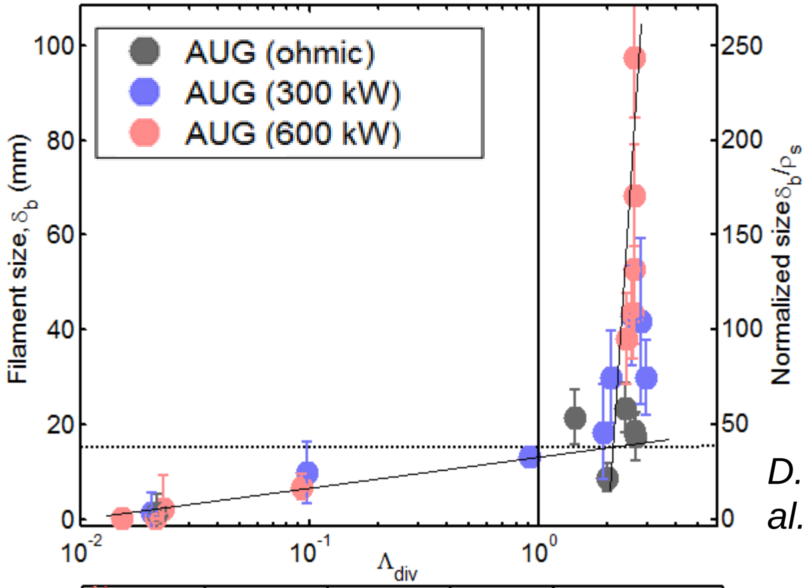

D. Carralero et al., PRL, (2015)

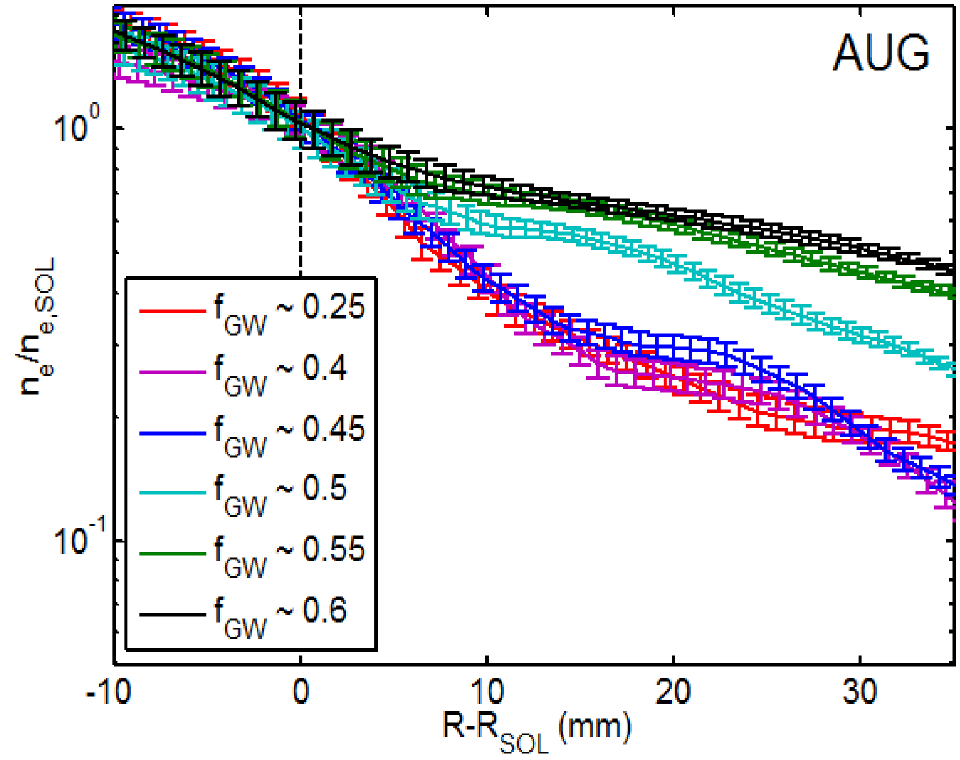

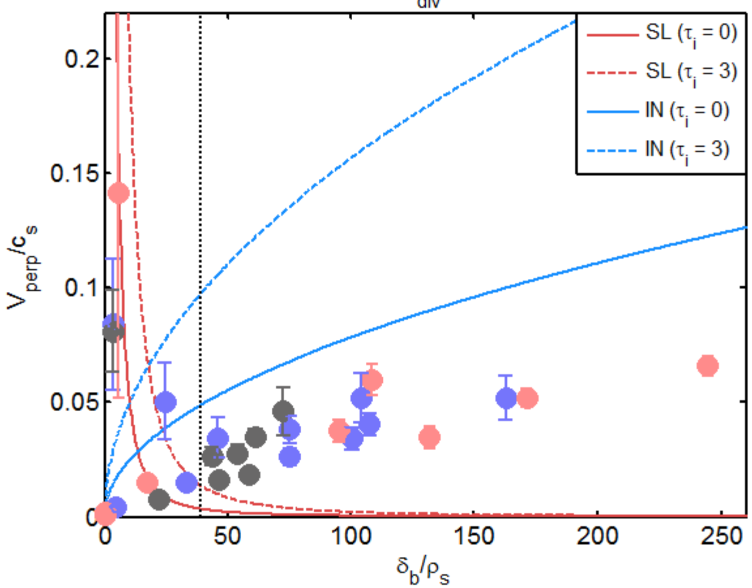

$$\Lambda = \frac{L_\parallel / c_s}{1/\nu_{ei}} \frac{\Omega_i}{\Omega_e} \simeq \frac{\tau_\parallel}{\tau_{ei}}$$

J.R. Myra et al., PoP, (2006)

Filaments and Shoulder

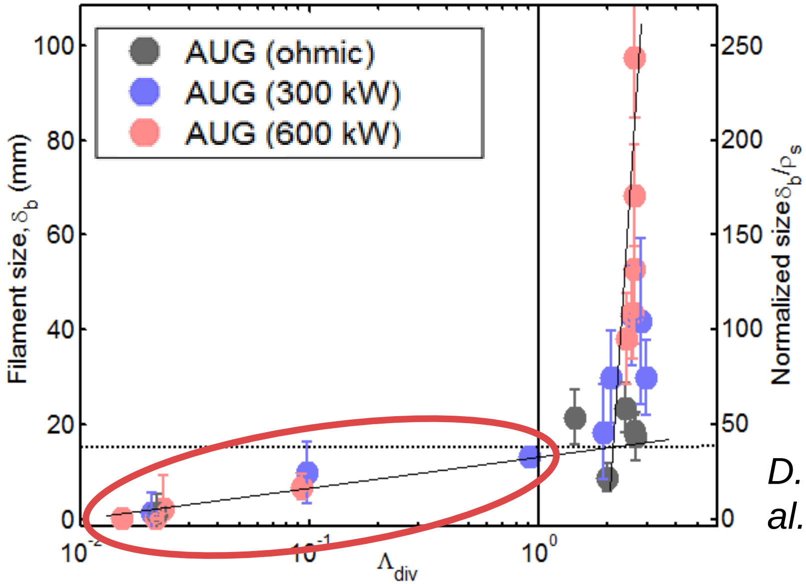

D. Carralero et al., PRL, (2015)

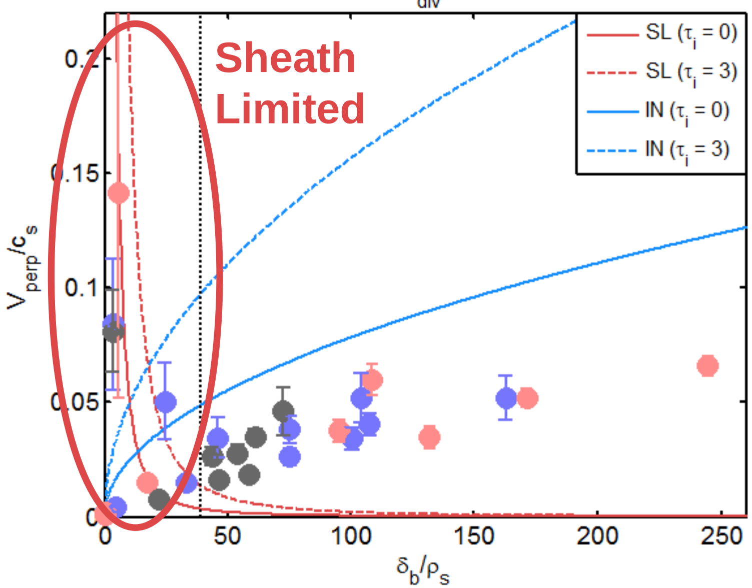

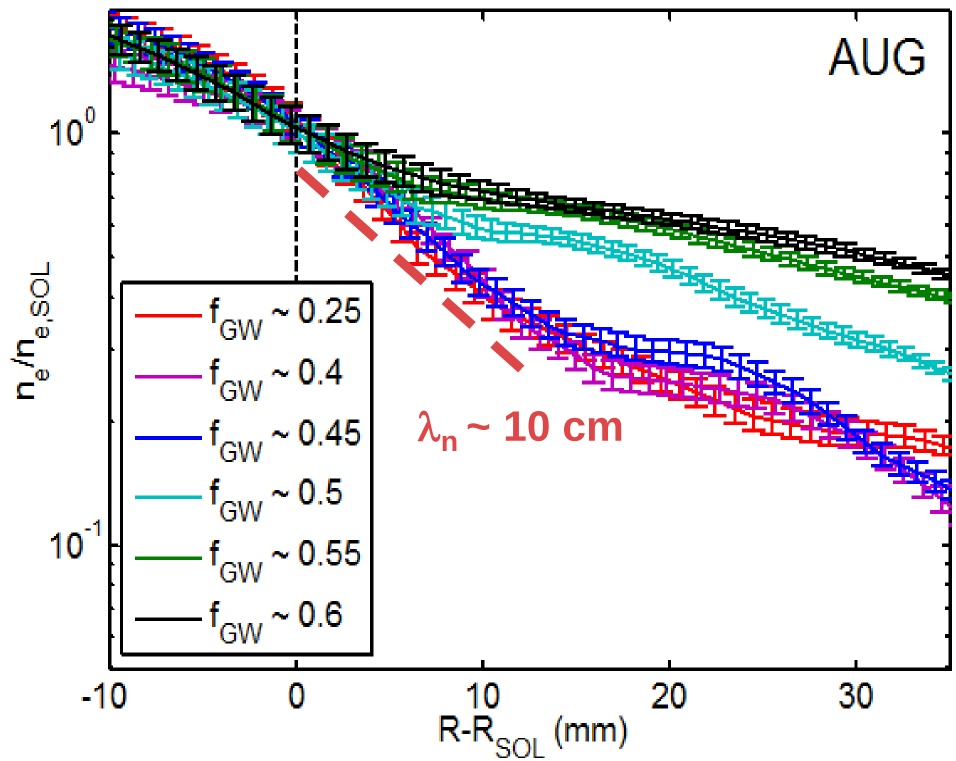

$$\Lambda = \frac{L_\parallel / c_s}{1/\nu_{ei}} \frac{\Omega_i}{\Omega_e} \simeq \frac{\tau_\parallel}{\tau_{ei}}$$

J.R. Myra et al., PoP, (2006)

$$\Lambda < 1$$

$$v_b^{SL} = c_s(1+\tau_i)\frac{L_\parallel}{R}\frac{\tilde{n}}{\bar{n}+\tilde{n}}\left(\frac{\rho_s}{\delta_b}\right)^2$$

Filaments and Shoulder

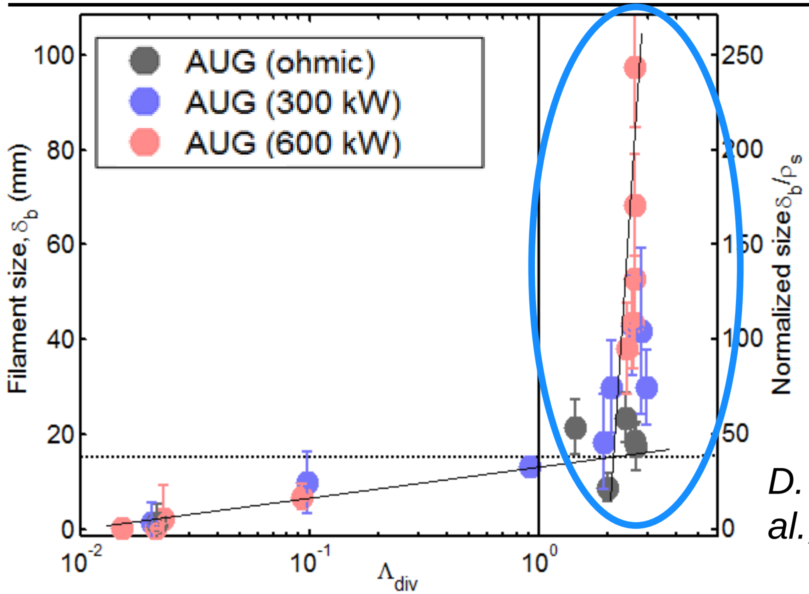

D. Carralero et al., PRL, (2015)

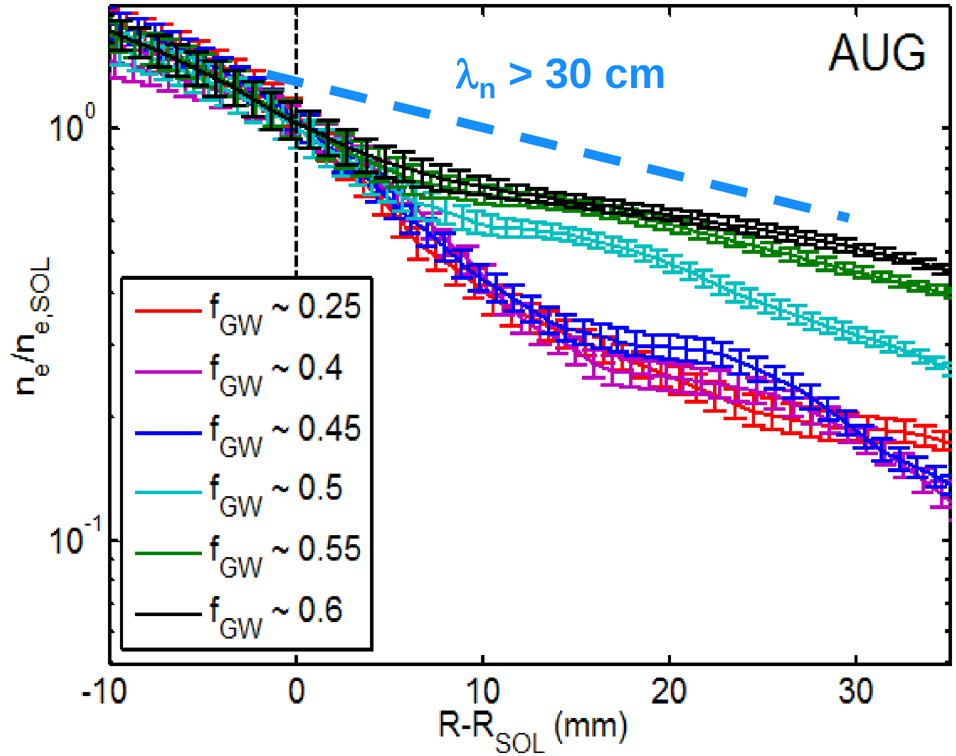

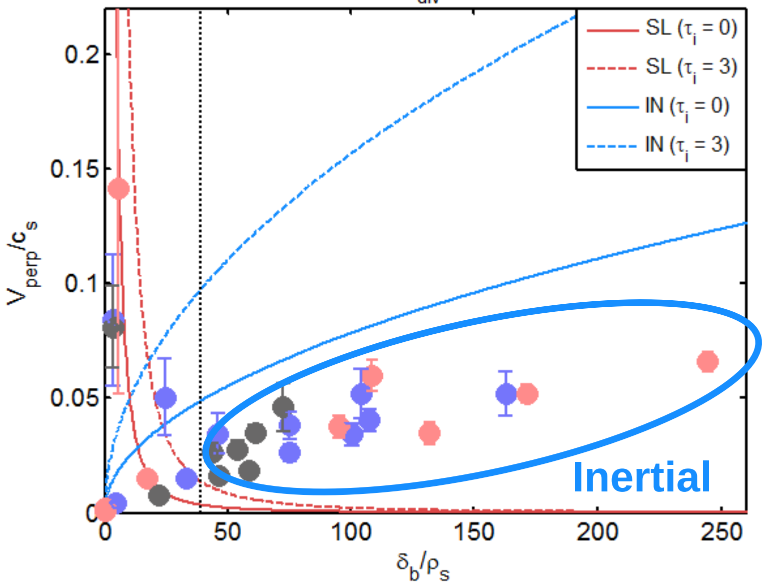

$$\Lambda = \frac{L_\parallel / c_s}{1/\nu_{ei}} \frac{\Omega_i}{\Omega_e} \simeq \frac{\tau_\parallel}{\tau_{ei}}$$

J.R. Myra et al., PoP, (2006)

$$\Lambda > 1$$

$$v_b^{IN} = c_s \sqrt{(1+\tau_i)\frac{\tilde{n}}{\bar{n}+\tilde{n}}\frac{\delta_b}{R}}$$

Filaments and Shoulder

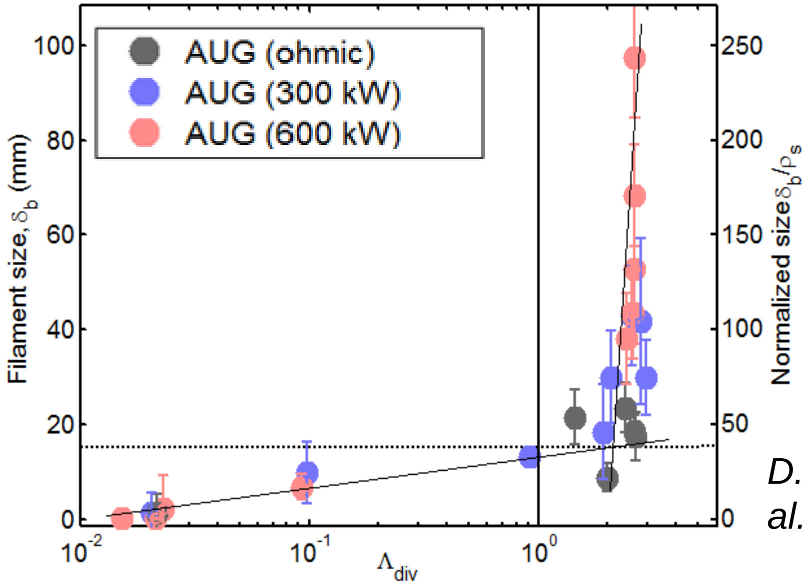

D. Carralero et al., PRL, (2015)

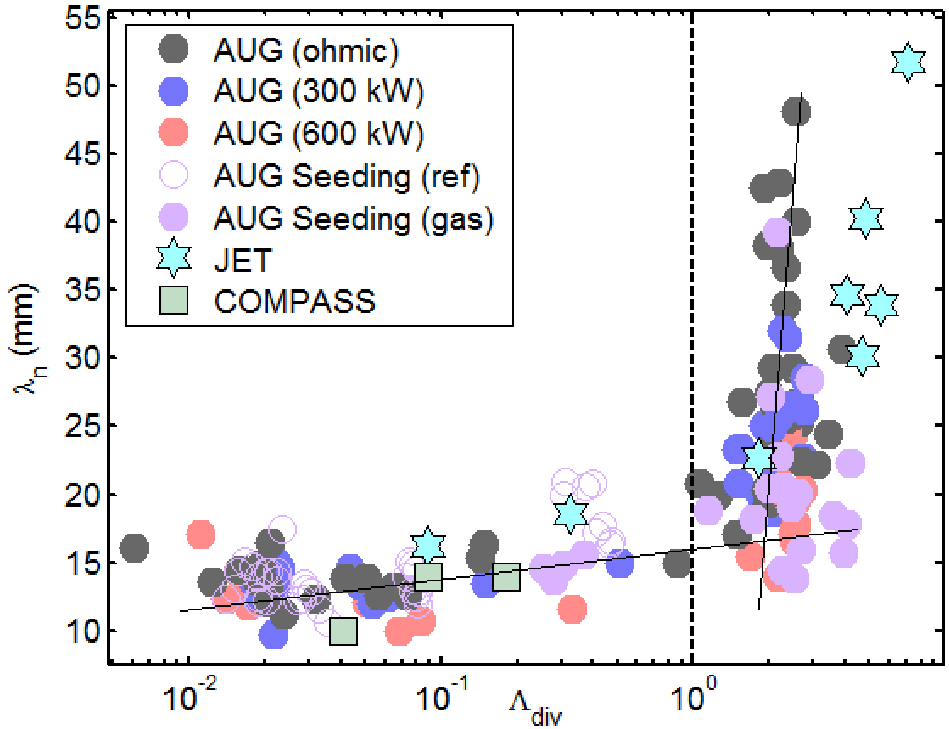

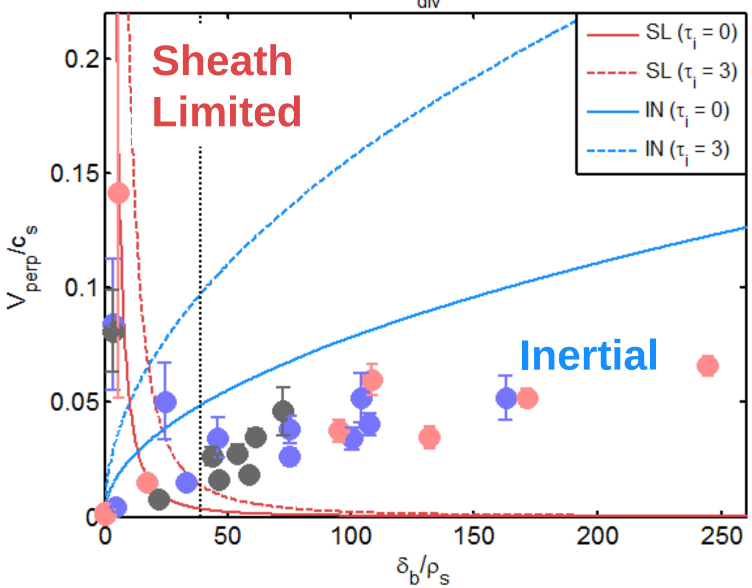

Λ_{div} scaling of the shoulder formation **has been demonstrated** on the COMPASS-AUG-JET ITER Stepladder

Evolution of particle transport

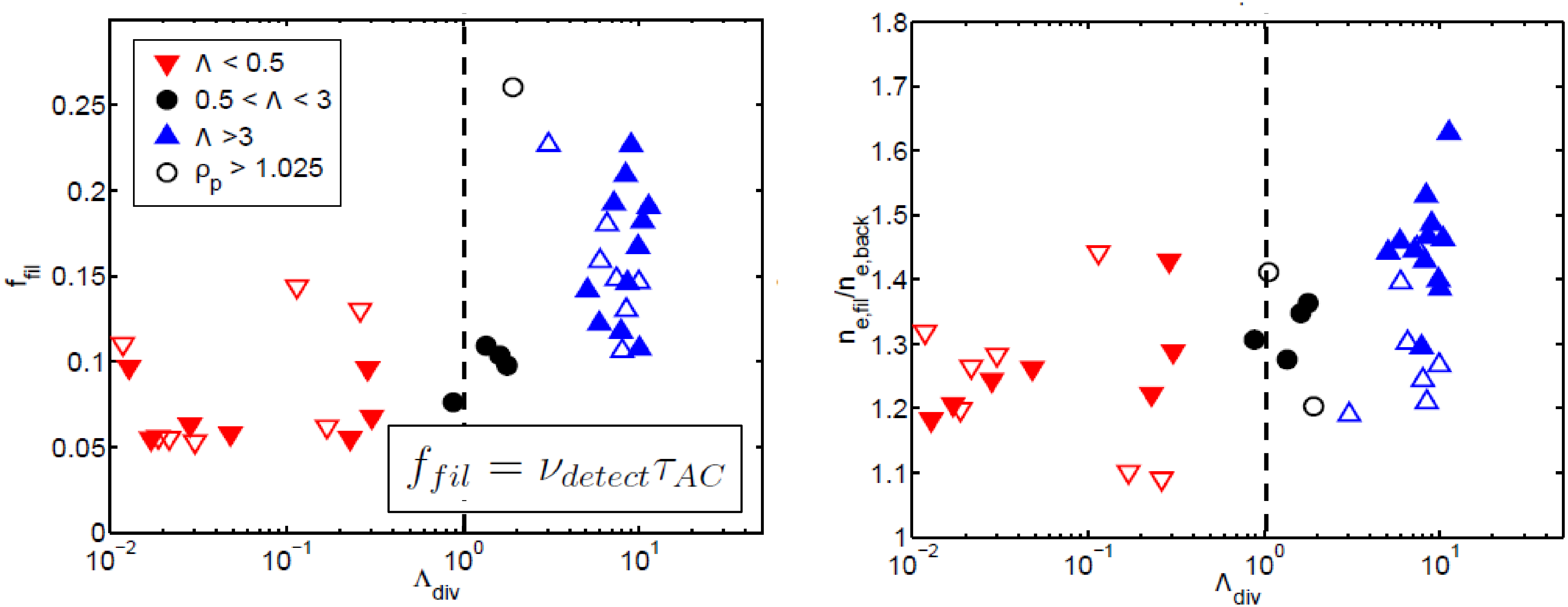

The filament transition has clear effects on filamentary transport:

- Packing fraction, f_{fil} and amplitude of fluctuations n_{fil}/n_{back} **substantially increased**

Evolution of particle transport

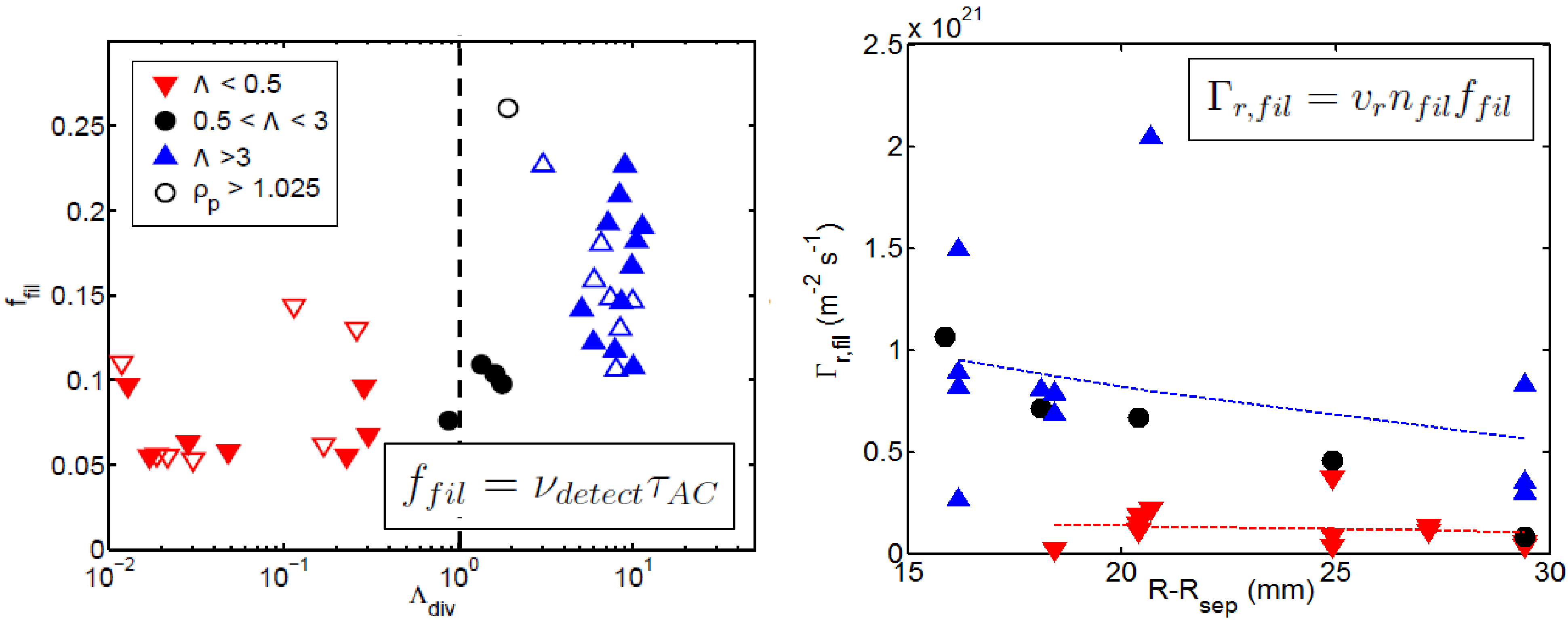

The filament transition has clear effects on filamentary transport:

- Packing fraction, **f_{fil}** and amplitude of fluctuations **n_{fil}/n_{back} substantially increased**
- **Γ_r** across the separatrix **is increased by a factor 3-4**
- Simmilar results reported from JET (Guillemaut PSI 2016)

Thermal evolution of the SOL

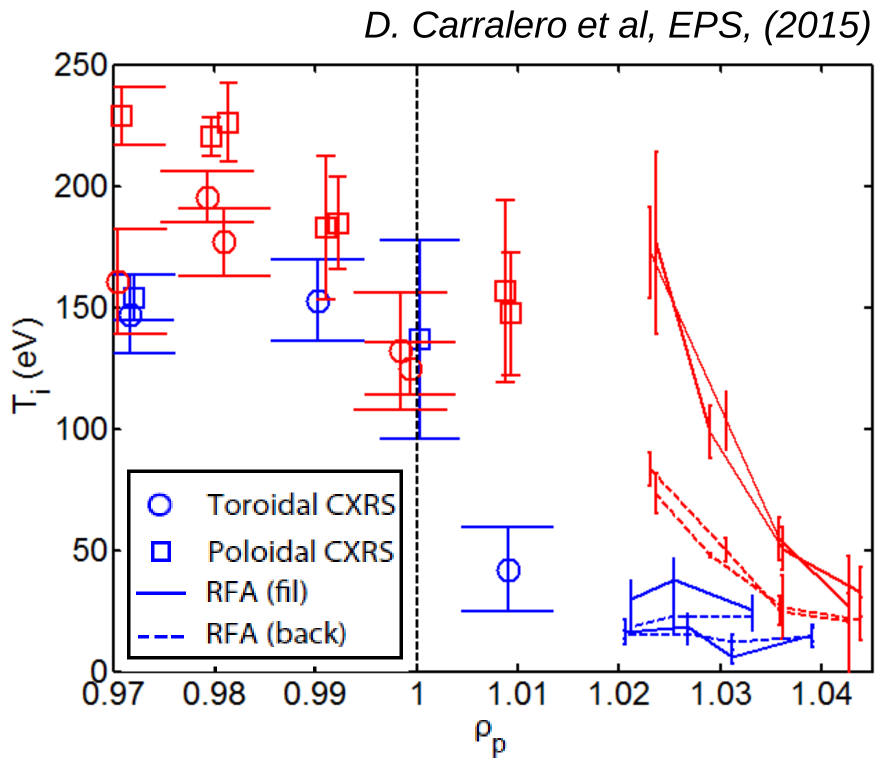

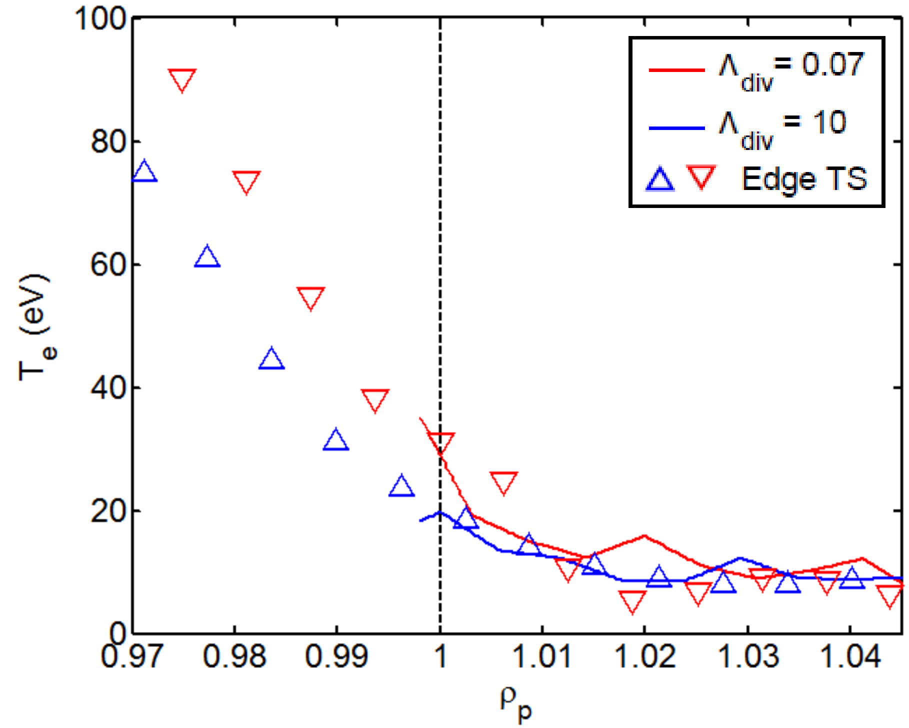

Electrons and ions show very different behaviour through the transition:

- $T_{e,fil} \sim 1.2\, T_{e,back}$, **$T_e$ roughly constant** across the SOL.
- $T_{i,fil} > T_{i,back}$ for $\Lambda_{div} < 1$. Slow radial decay, **$\lambda_{Ti} \sim 40$ mm**.
- $T_{i,fil} \sim T_{i,back} \sim 25$ eV for high $\Lambda_{div} > 1$. Fast radial decay, **$\lambda_{Ti} \sim 10$ mm**.

Evolution of heat transport

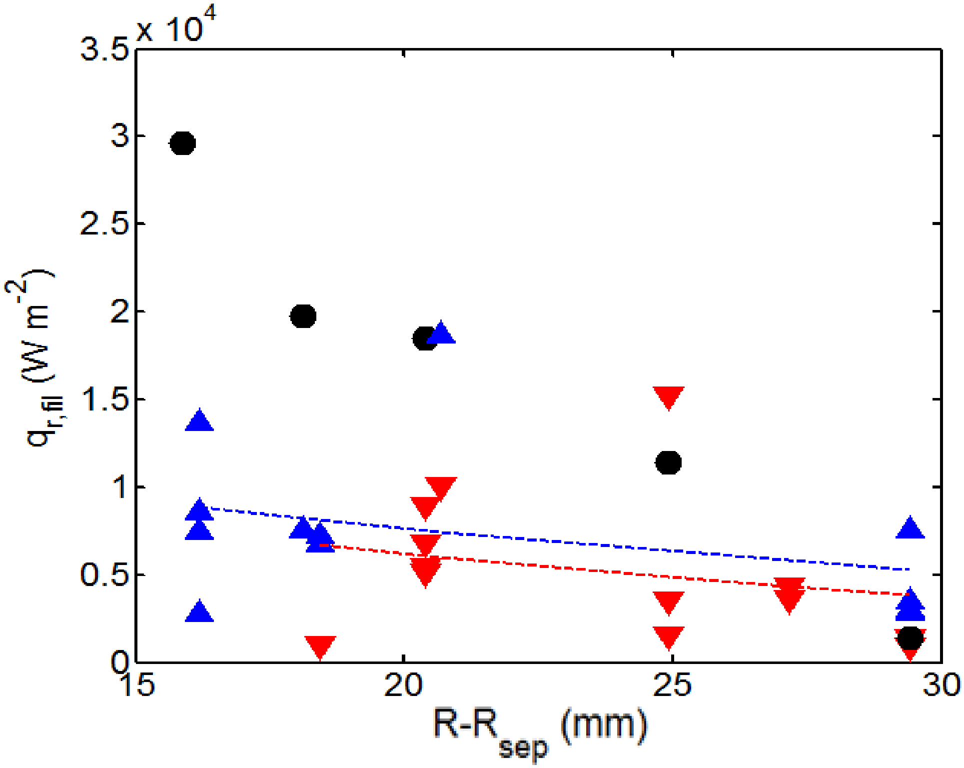

D. Carralero et al, in preparation, (2016)

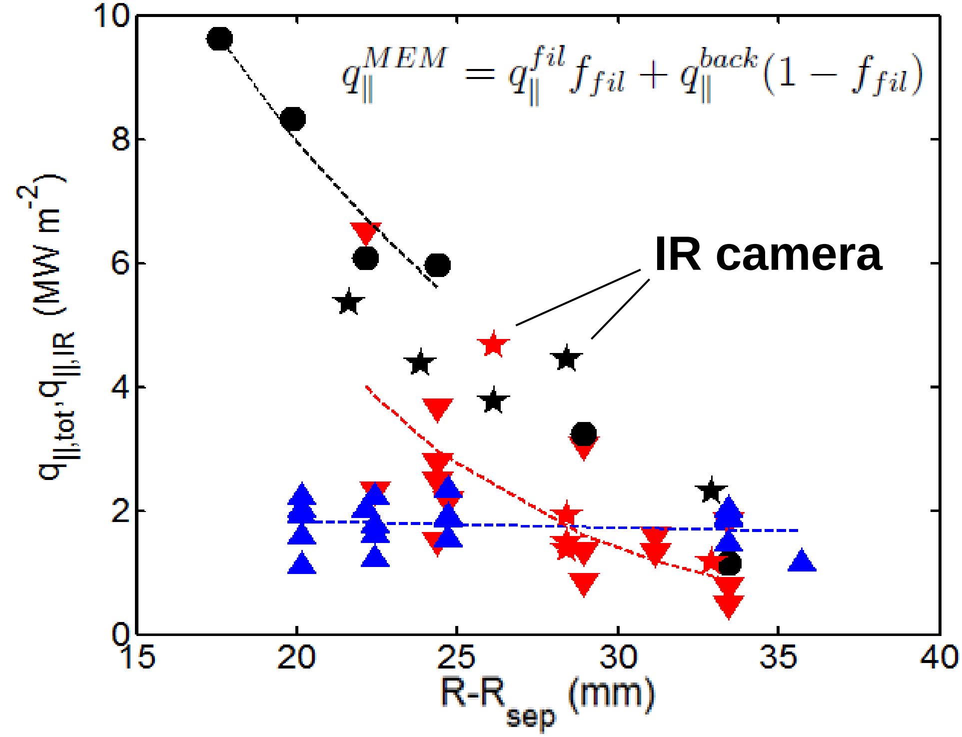

Heat transport is not affected by the transition

- $q_{r,fil}$ near the wall are simmilar. Agreement with JET (Guillemaut, PSI 2016)
- A maximum in $q_{r,fil}$ is reached around the transition.
- Good agreement with IR measurements of the $q_{||}$ at the manipulator.

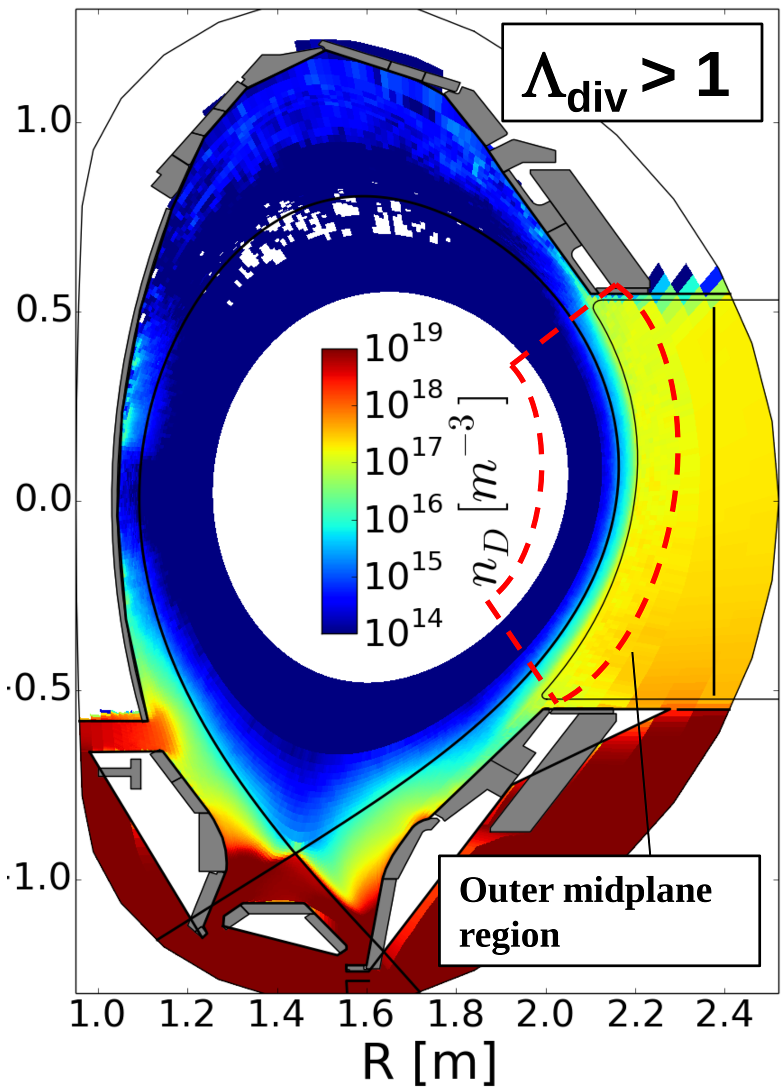

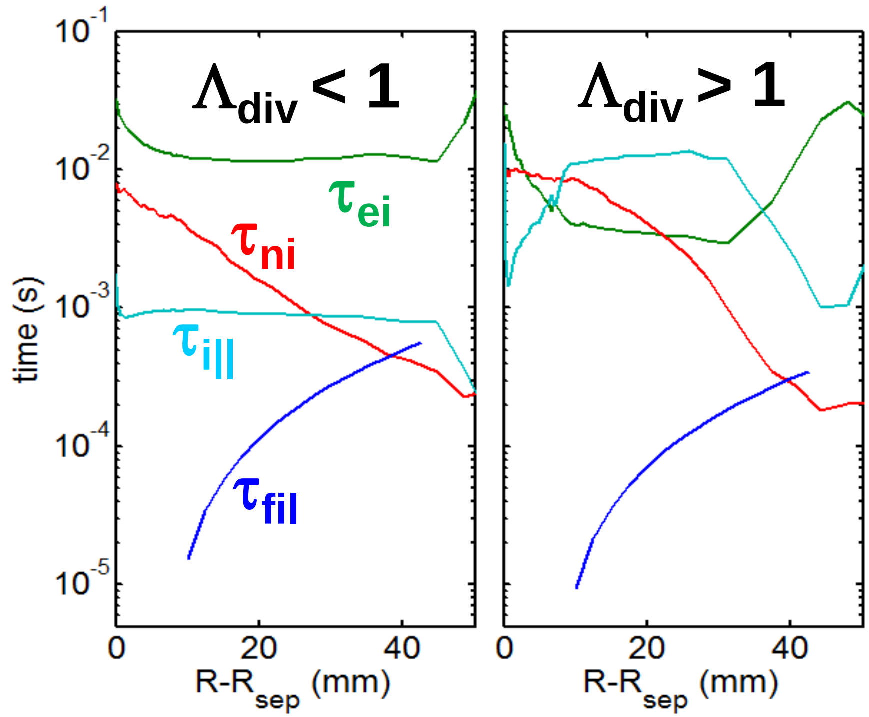

$$\tau_{ie}^{-1} \simeq \frac{m_e}{m_i}\nu_{ie}\frac{T_i - T_e}{T_i}$$

$$\tau_{in}^{-1} \simeq \nu_{in}\frac{T_i - T_n}{T_n}$$

$$\tau_{i||}^{-1} \simeq \frac{T_i}{m_i \nu_{ii}}\frac{1}{L_{||}^2}$$

$$\tau_{fil}^{-1} \simeq \frac{R - R_{SOL}}{v_{\perp,fil}}$$

EMC3-EIRENE code is used to simulate $\Lambda_{div} > 1$ and $\Lambda_{div} < 1$ scenarios

- **No thermalization** mechanism can reduce T_i as observed in the experiment.

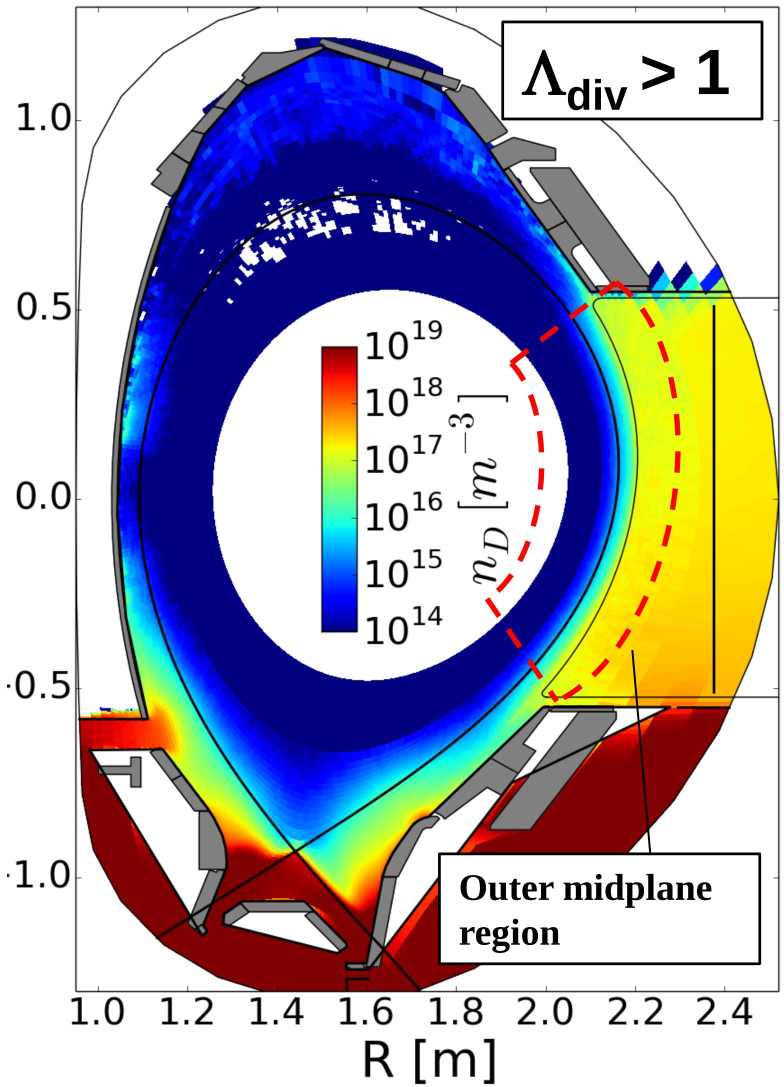

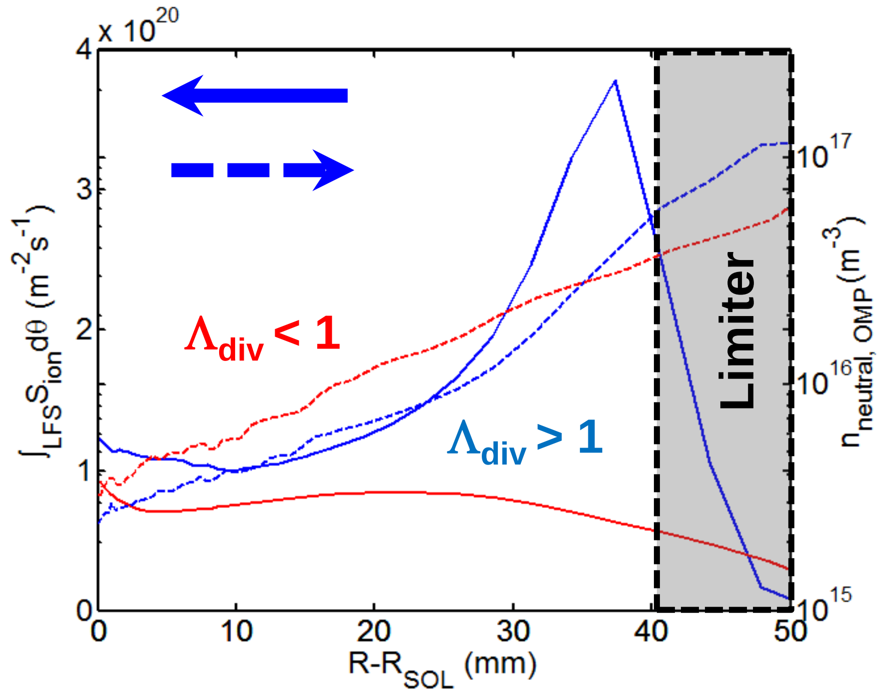

EMC3-EIRENE code is used to simulate $\Lambda_{div} > 1$ and $\Lambda_{div} < 1$ scenarios

- **No thermalization** mechanism can reduce T_i as observed in the experiment.
- An **ionization front** builds **in front of the limiter** shadow in the $\Lambda_{div} > 1$ case.

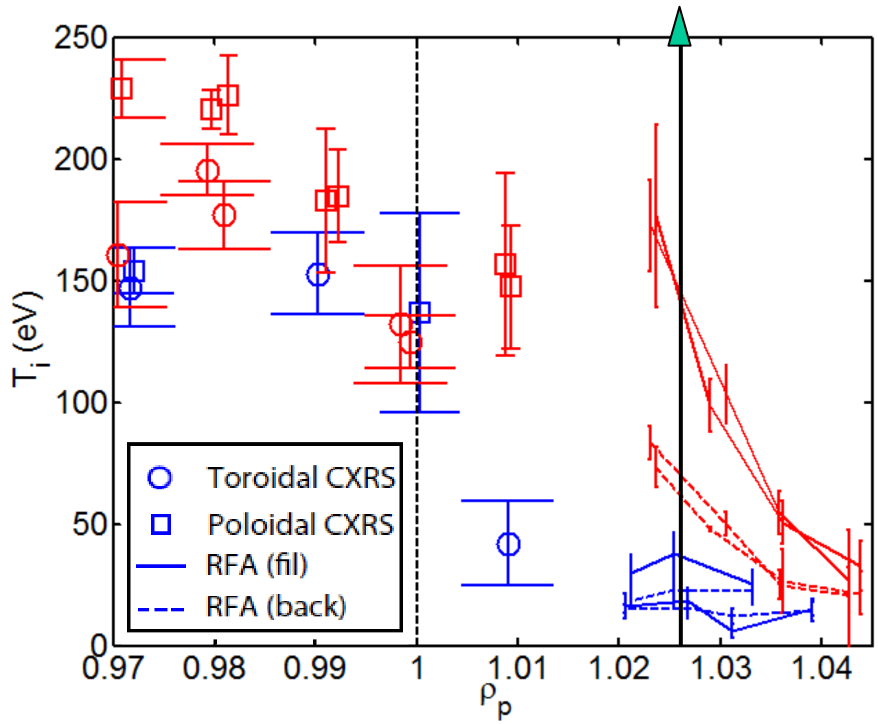

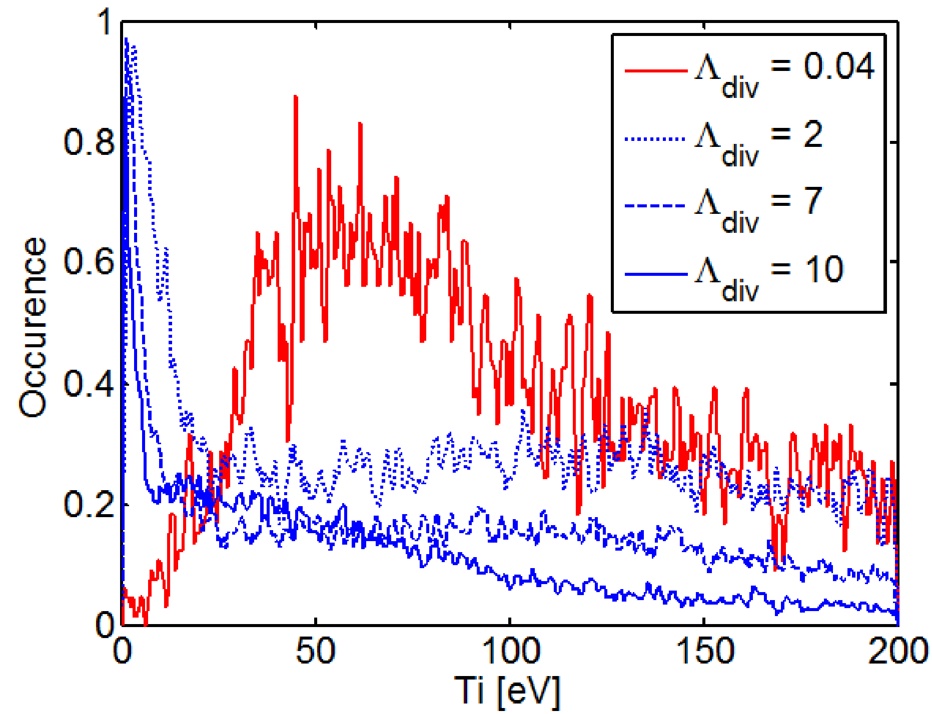

ExB analyzer experiments are consistent with RFA measurements :

- $\Lambda_{div} < 1 \rightarrow$ **Monoenergetic distribution** with a positive tail, consistent with $T_{i,back}$ and $T_{i,fil}$.
- $\Lambda_{div} > 1 \rightarrow$ **Two-energies distribution** with cold ions around the F.C. $T_{i,fil}$ not necessarily greater than $T_{i,back}$.

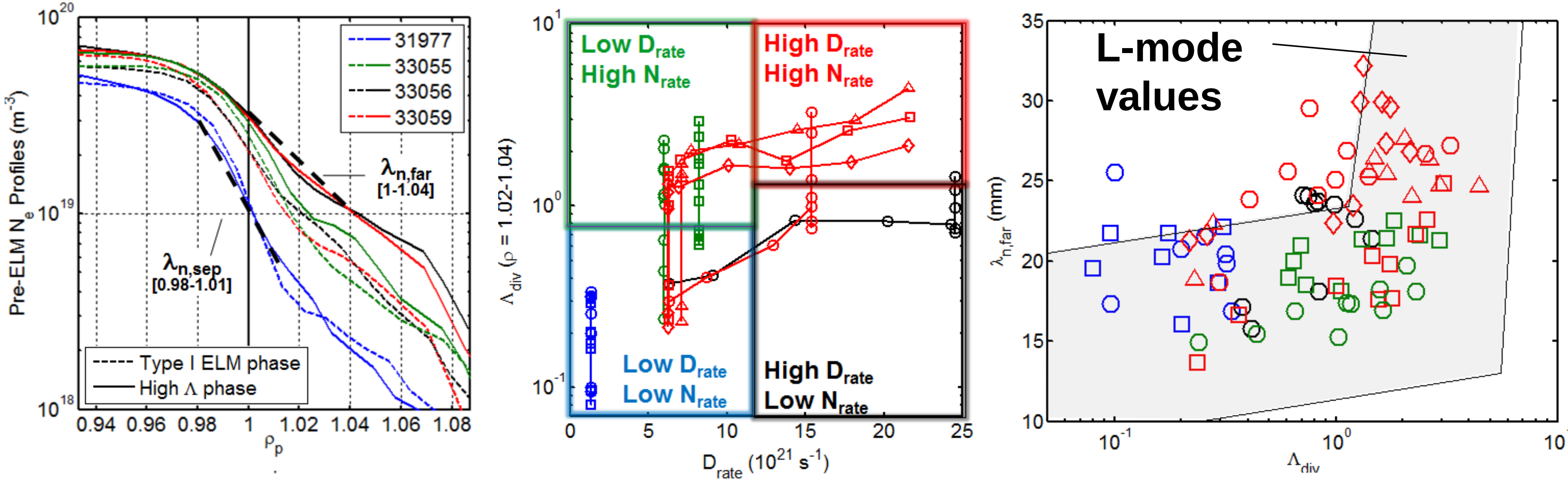

D. Carralero et al, PSI, (2016)

Equivalent experiments have analyzed the shoulder formation on inter-ELM H-mode plasma:

- **A simmilar shoulder** has been observed.
- An **equivalent filament transition** takes place for $\Lambda_{div} > 1$
- $\Lambda_{div} > 1$ is a necessary but not sufficient condition. **A minimum level of D fueling is also required.** This is consistent with L-mode experiments in TCV [N. Vianello, this conference, EX/P8-26].

Looking ahead: DEMO

Several scenarios can be proposed for DEMO:

Standard (Extrapolation of current results):

$\lambda_{Ti} \sim 10$ mm, $\lambda_n \sim 40$ mm;

$1/\lambda_{q,i} \sim 1/\lambda_{Ti} + 1/\lambda_n \sim 10$ mm

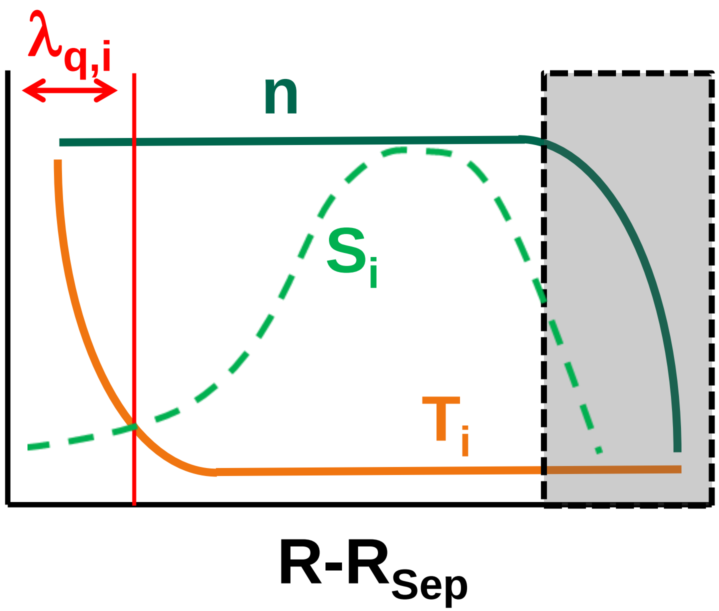

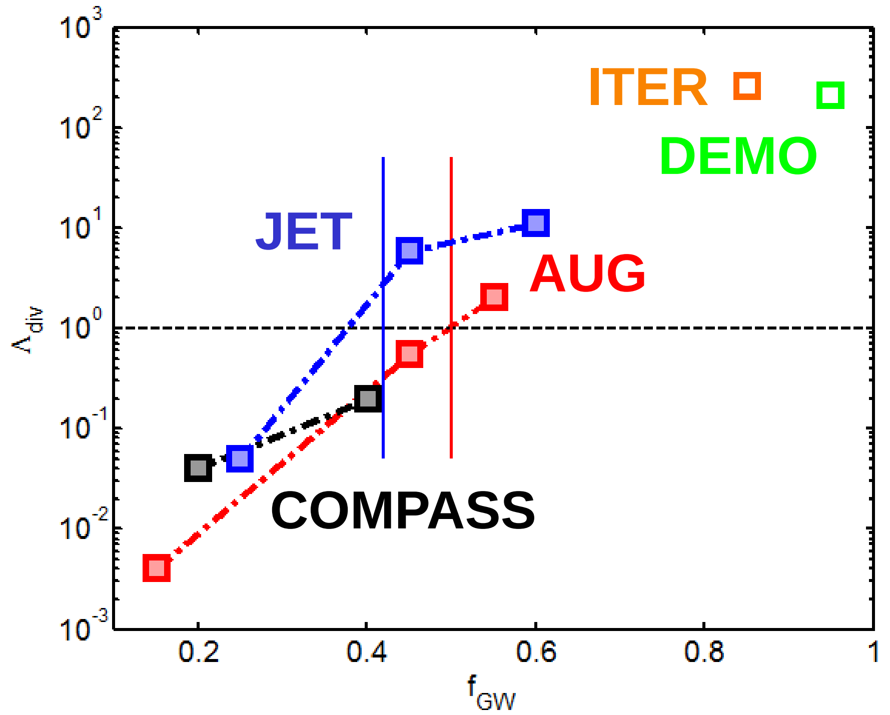

$\Lambda_{div} > 1$ ► Shoulder formation

$\lambda_i \sim R_w - R_{Sep}$ ► $\lambda_{Ti} << R_w - R_{sep}$

$\lambda_{q,i} << R_w - R_{Sep}$ ► High divertor load

$T_{i,wall} \sim 10\text{-}20$ eV ► Low wall sputtering

Looking ahead: DEMO

Several scenarios can be proposed for DEMO:

Worst case (No shoulder formation):

$\lambda_{Ti} \sim 40$ mm, $\lambda_n \sim 10$ mm;

$1/\lambda_{q,i} \sim 1/\lambda_{Ti} + 1/\lambda_n \sim 10$ mm

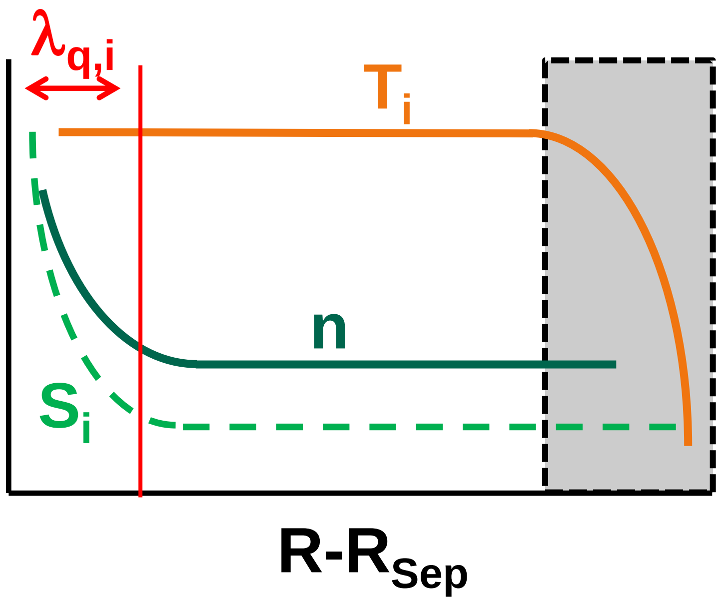

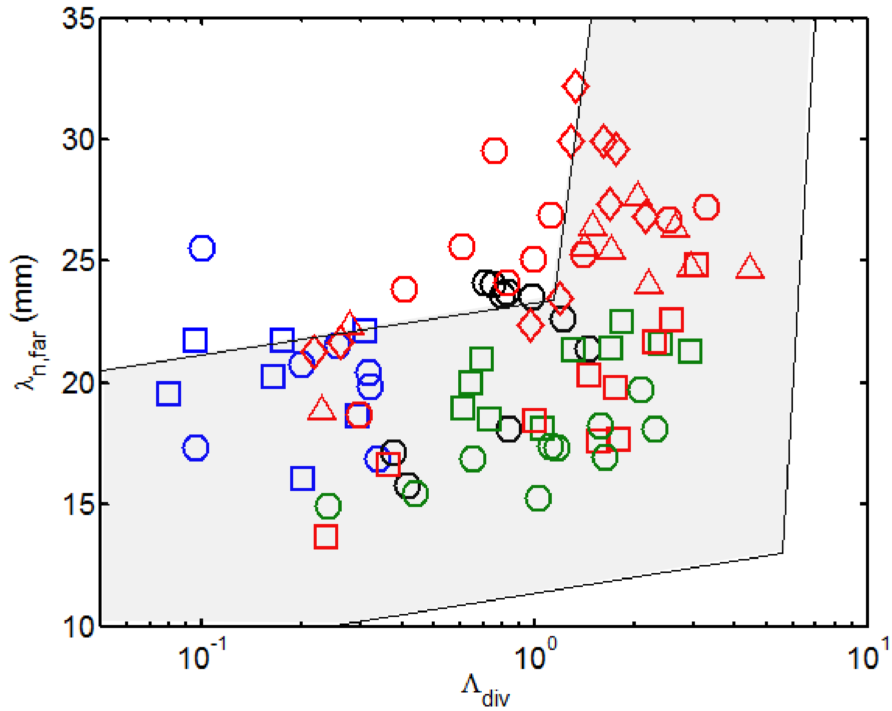

Insufficient n_n in the SOL

$\lambda_i >> R_w\text{-}R_{Sep}$ ► $\lambda_{Ti} \sim R_w\text{-}R_{sep}$

$\lambda_{q,i} << R_w\text{-}R_{Sep}$ ► High divertor load

$T_{i,wall} >> 10\text{-}20$ eV ► High wall supttering

Looking ahead: DEMO

Several scenarios can be proposed for DEMO:

Best case (independent shoulder formation/ion cooling, widened near-SOL):

$$\lambda_{Ti} \sim 40 \text{ mm}, \lambda_n \sim 40 \text{ mm};$$

$$1/\lambda_{q,i} \sim 1/\lambda_{Ti} + 1/\lambda_n \sim 40 \text{ mm}$$

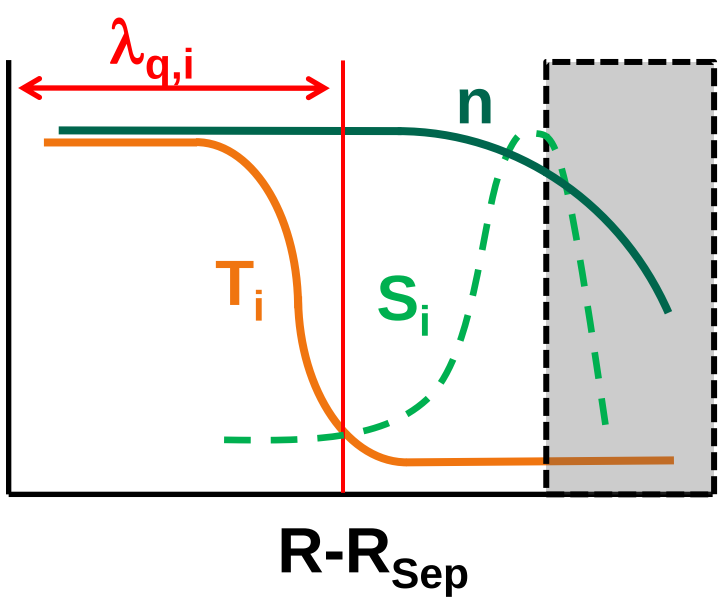

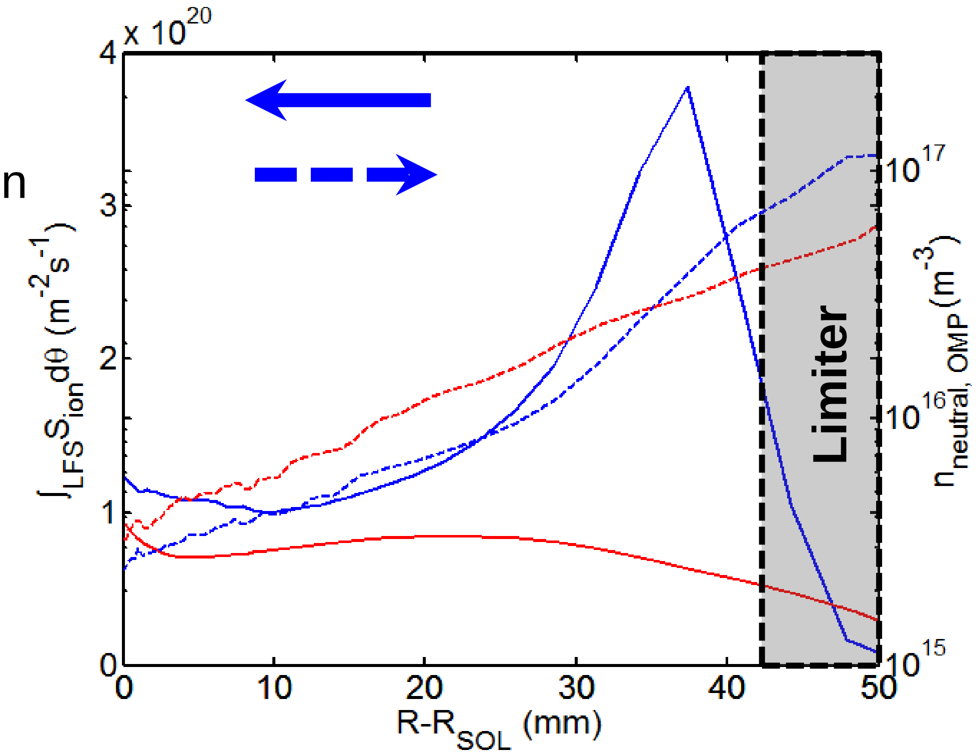

$\Lambda_{div} > 1$ ► Shoulder formation

$\lambda_i < R_w\text{-}R_{Sep}$ ► $\lambda_{Ti} < R_w\text{-}R_{Sep}$

$\lambda_{q,i} \sim R_w\text{-}R_{Sep}$ ► Low divertor load

$T_{i,wall} \sim$ 10-20 eV ► Low wall supttering

Summary and Conclusions

L-mode experiments on AUG, JET and COMPASS have shown the **relation between a filament transition and the shoulder formation**. This process is triggered by the **$\Lambda_{div} > 1$** thresshold.

The transition increases **Γ_{perp} by a factor 3** after the transition, while **q_{perp} remains roughly constant** due to the drop in T_i.

Simulations indicate that **ion cooling is not the result of thermalization**, but of the ionization of cold, recycled neutrals in front of the limiter. This is consistent with the **observation of a cold ion population for $\Lambda_{div} > 1$**.

H-mode experiments indicate **that a shoulder can form also between ELMs**. $\Lambda_{div} > 1$ is a necessary condition, but **sufficient D fueling level is also required.**

The shoulder is probably the result of a feedback loop between increased Γ_{perp}, wall recycling and ionization of reflected neutrals, leading to ever increased transport.

λ_{Te} and λ_{Ti} are decoupled, which could lead to enhanced λ_q under certain conditions in DEMO. Also, there is a risk of **high T_i D^+ ions arriving to the first wall.**

Additional Slides

A mechanism for shoulder formation

C. Guillemaut, et al., PSI Rome, (2016)

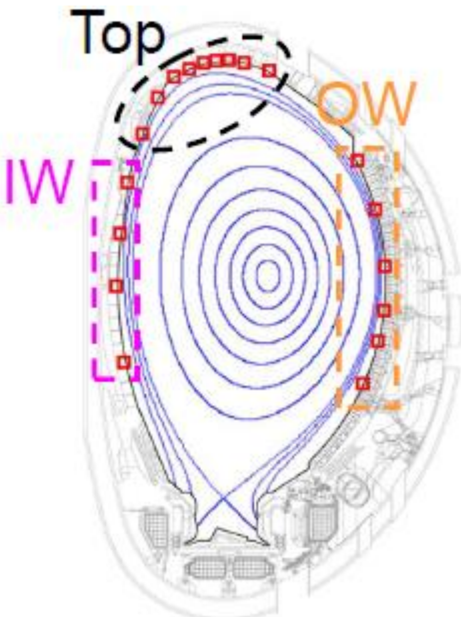

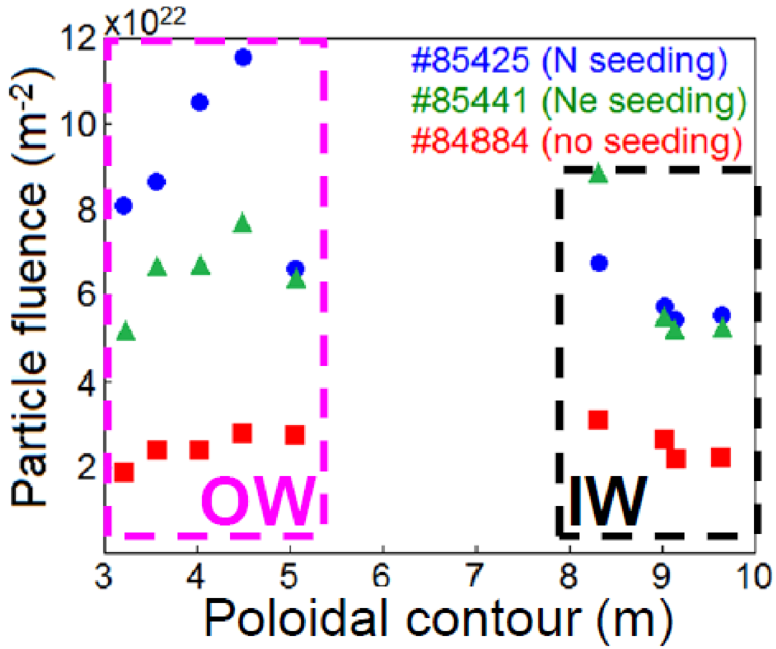

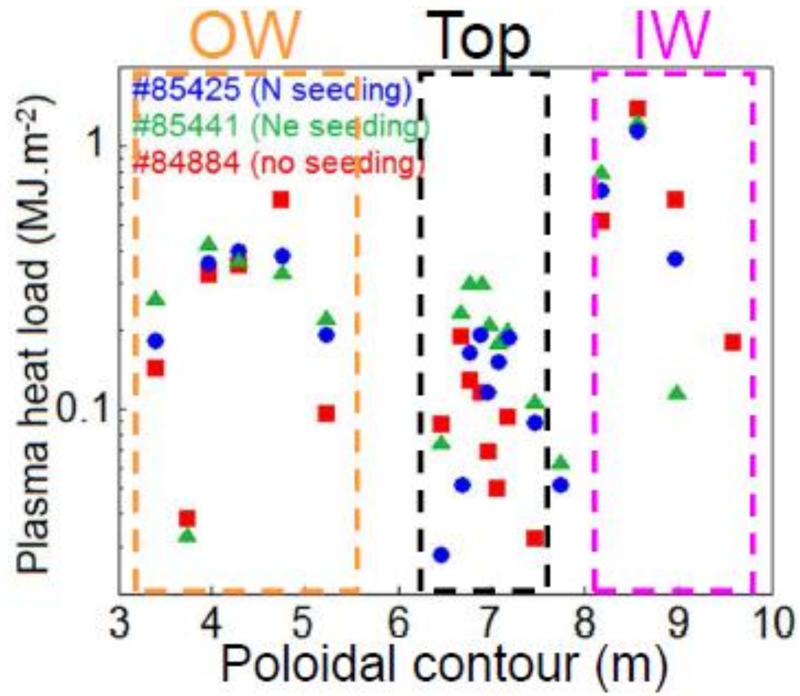

Evolution of particle transport

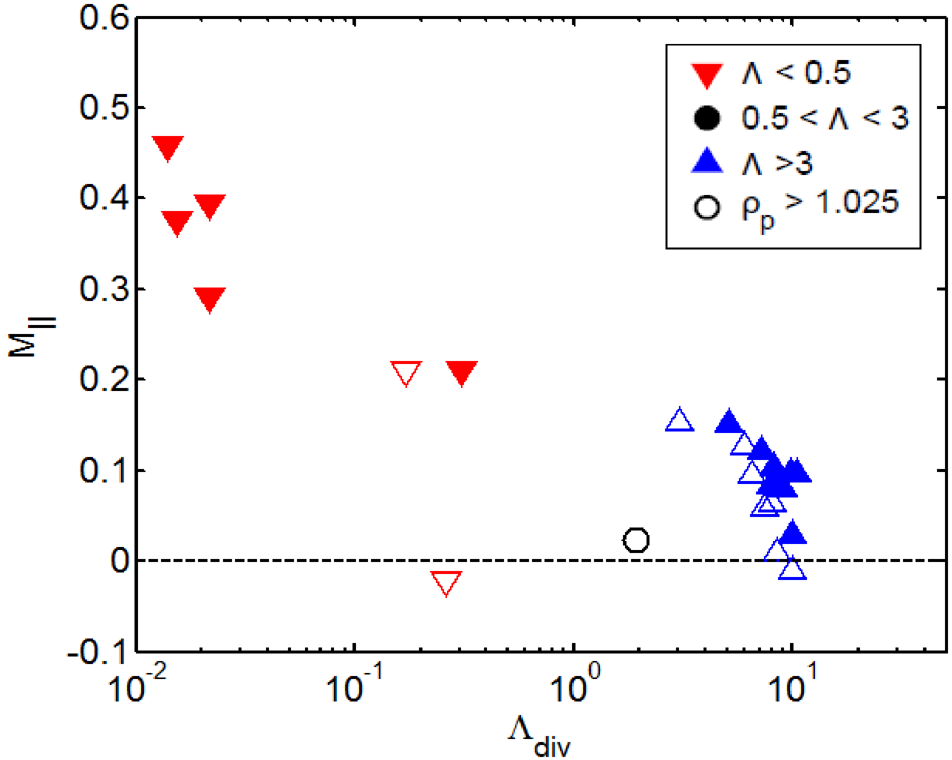

D. Carralero et al, in preparation, (2016)

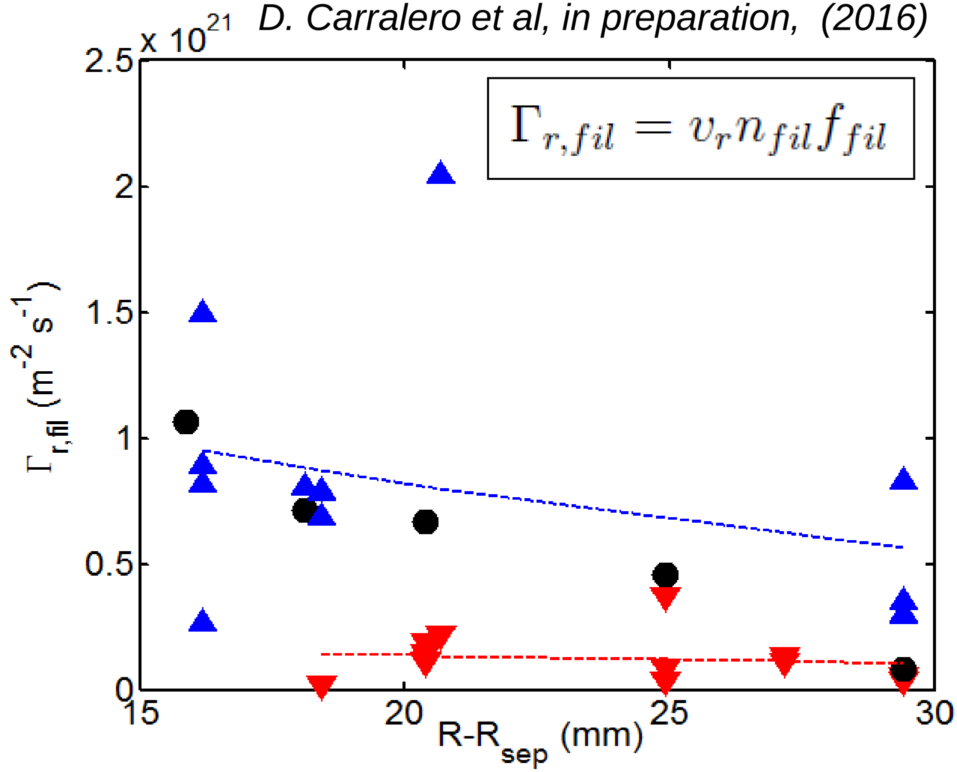

Evolution of heat transport

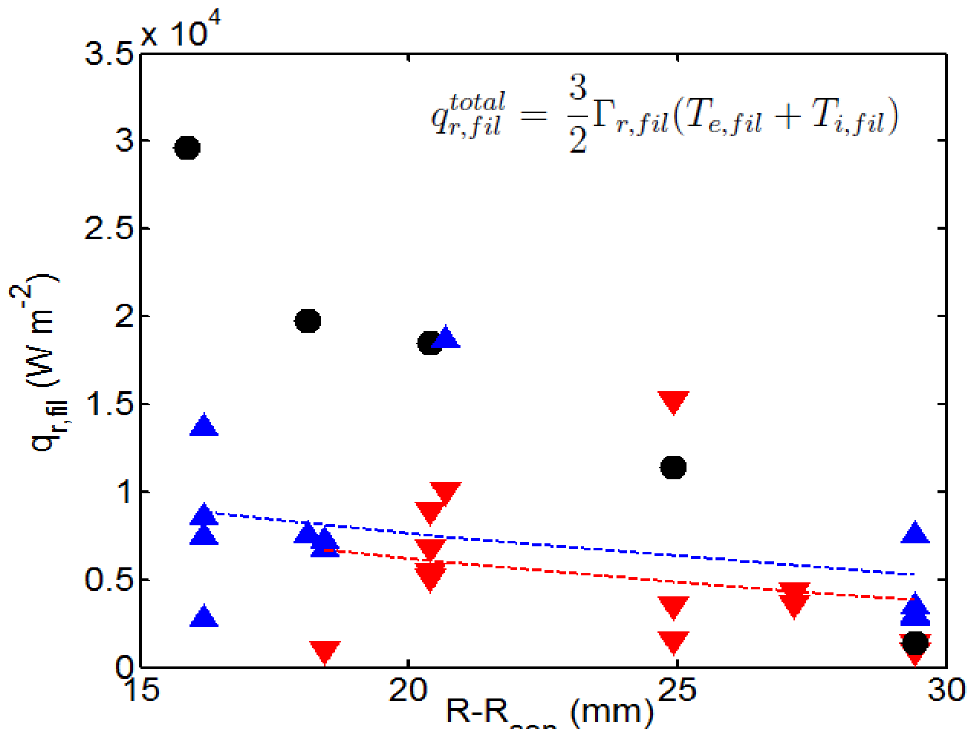

D. Carralero et al, in preparation, (2016)

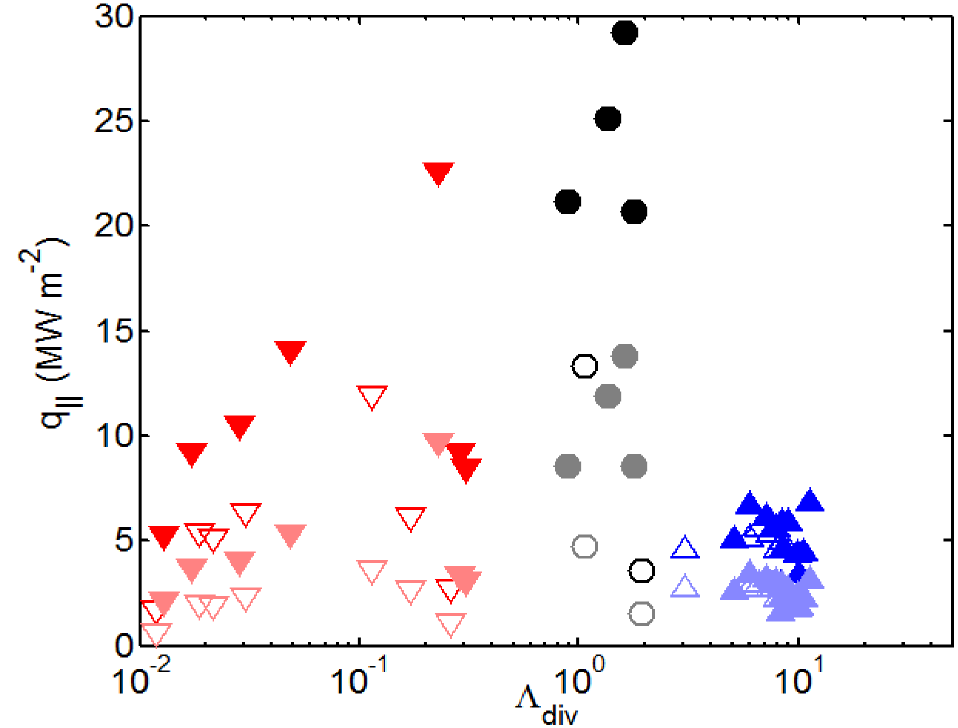

Validated by IR and JET

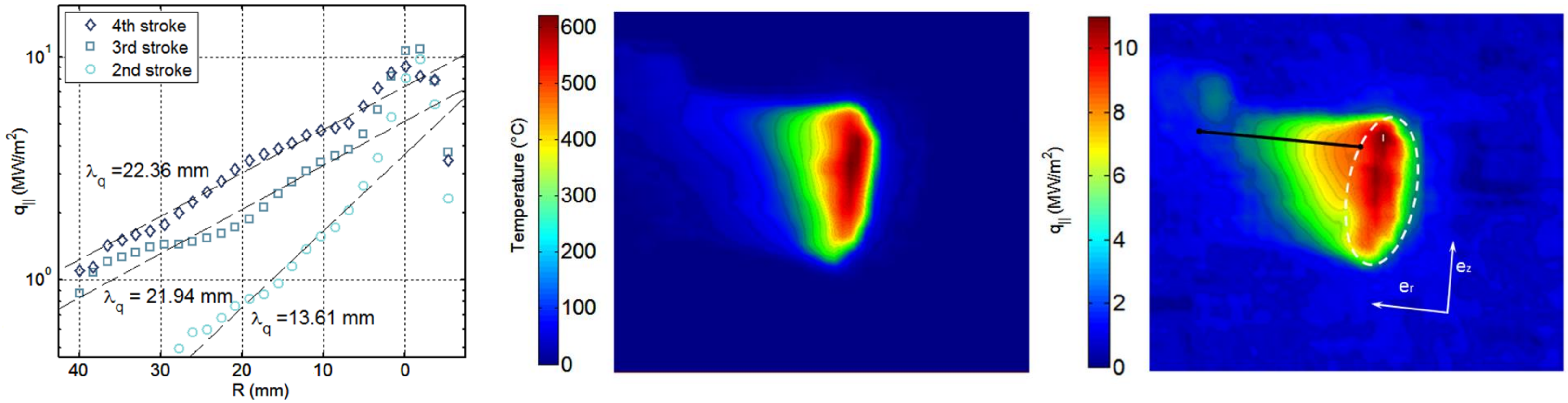

Total $q_{||}^{MEM}$ can be calculated and compared to IR measurements:

$$q_{||}^{MEM} = q_{||}^{fil} f_{fil} + q_{||}^{back}(1 - f_{fil})$$

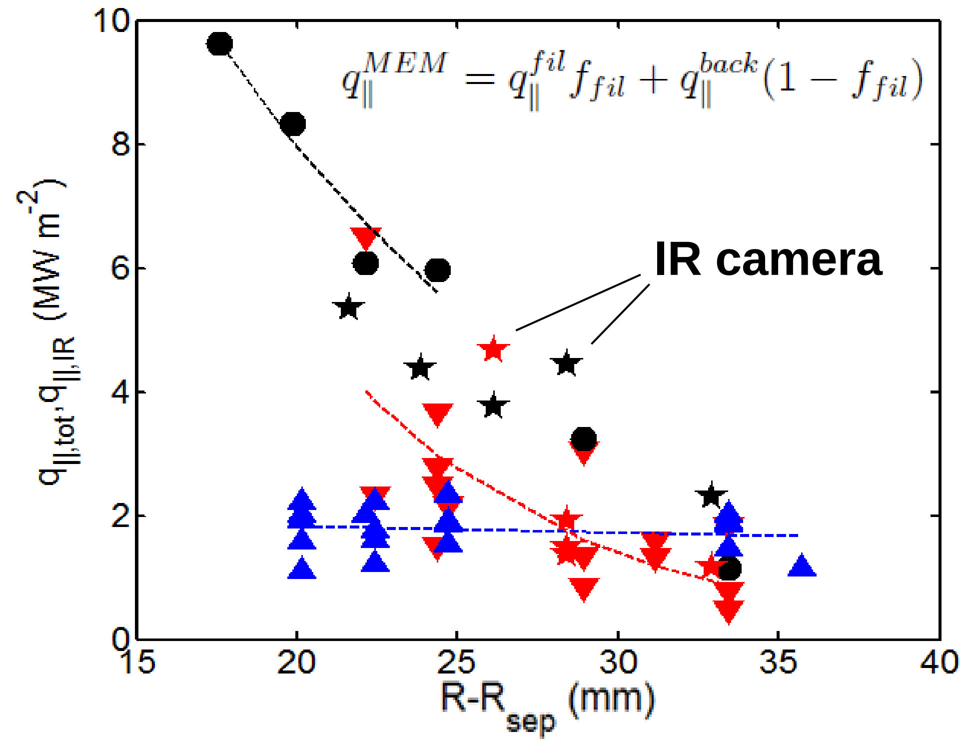

EMC3-EIRENE Simulations

$\Lambda_{div} < 1$

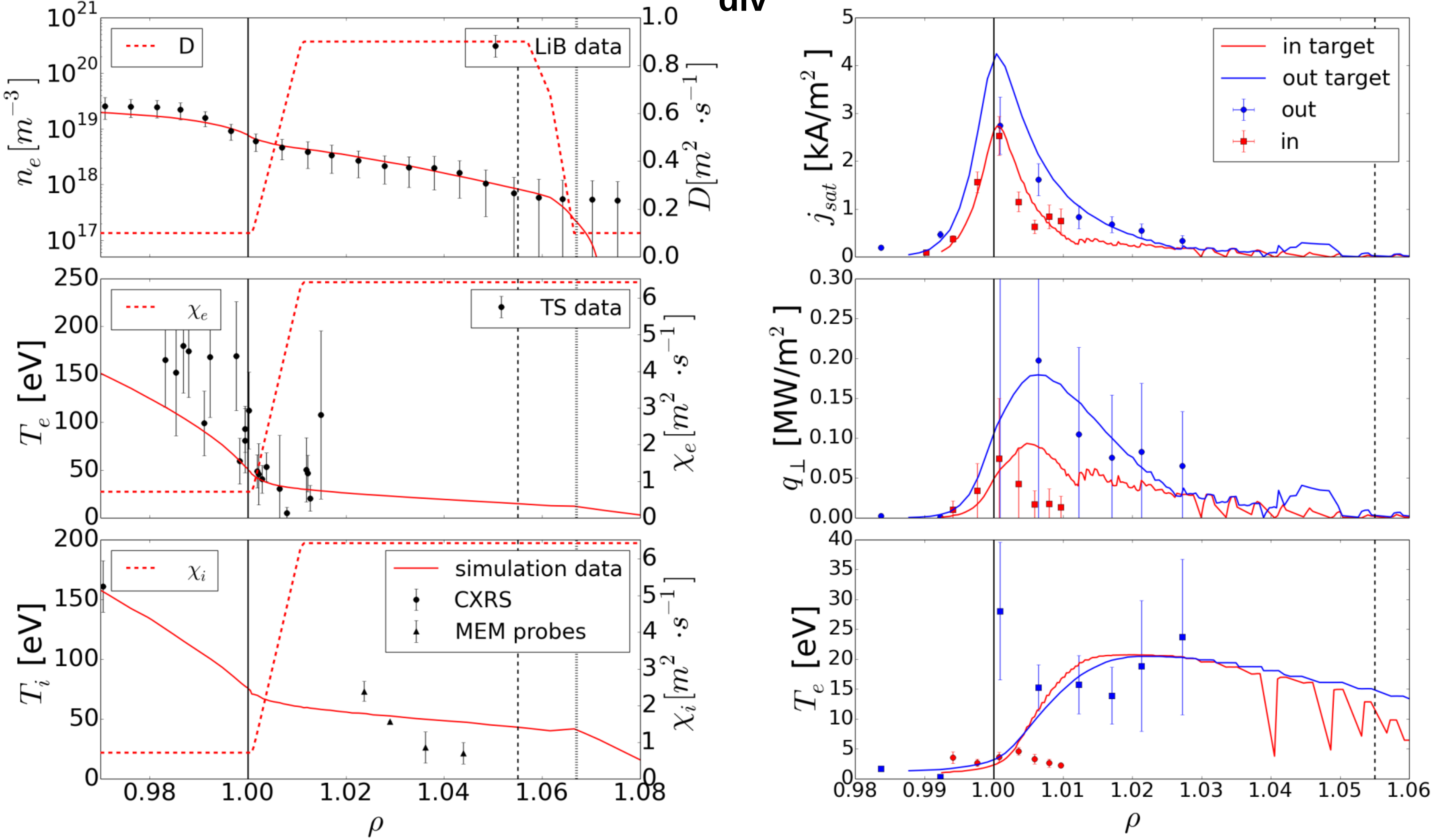

EMC3-EIRENE Simulations

$\Lambda_{div} > 1$

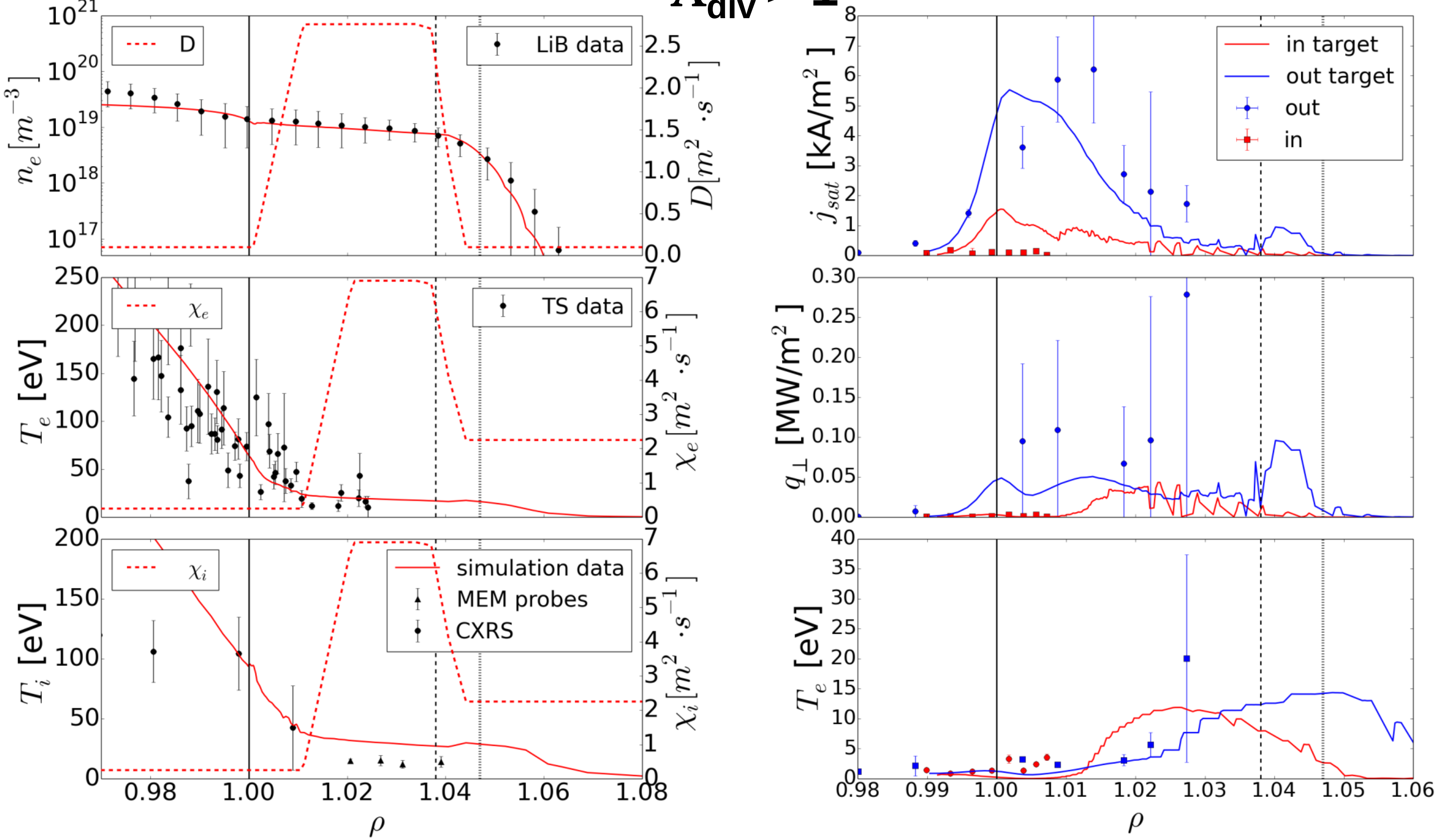

EMC3-EIRENE Simulations

Low density

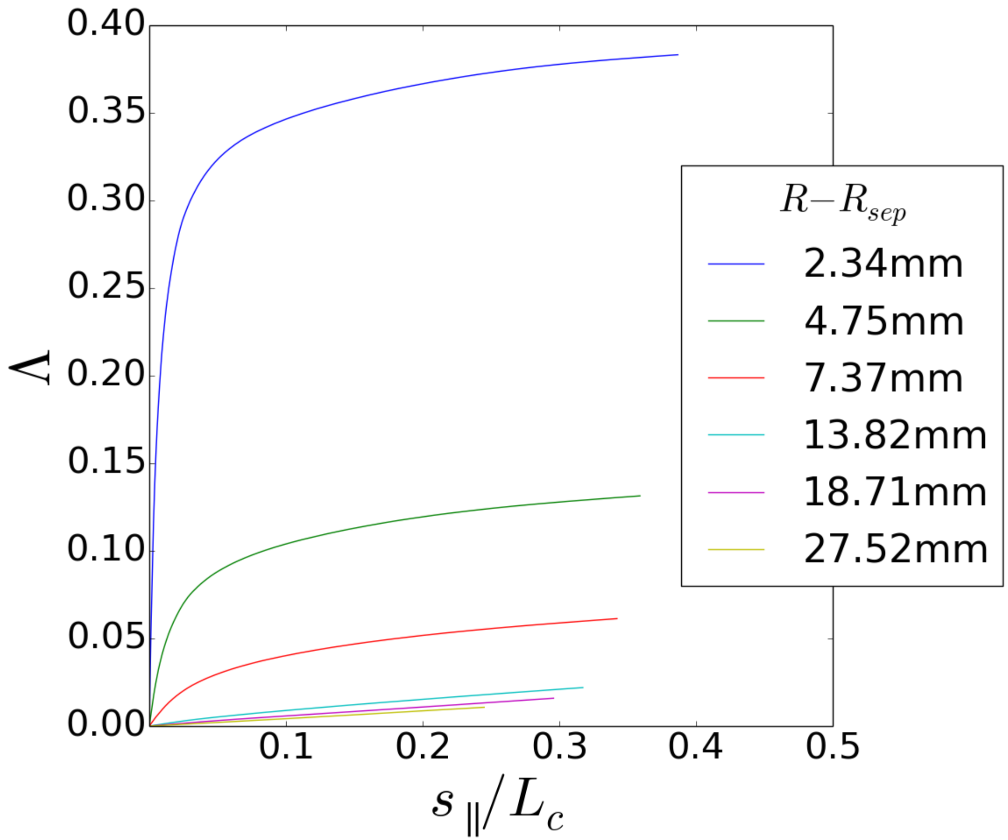

High density

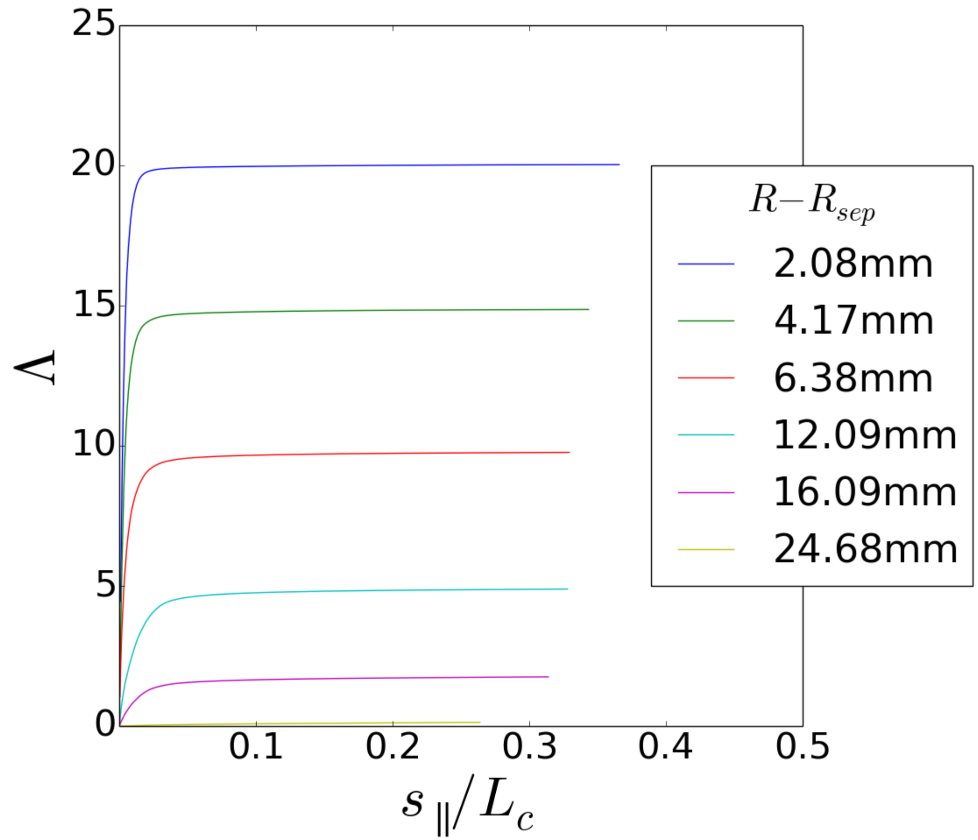

Probe head designed to measure ion energy distribution in real time.

Collaboration between AUG and COMPASS teams.

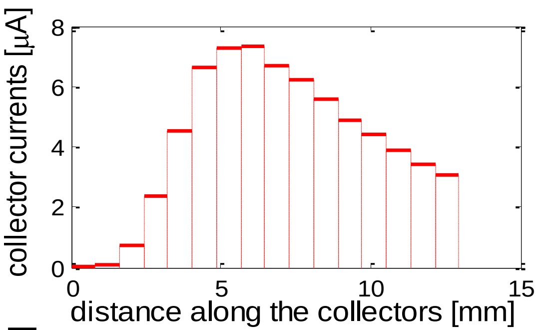

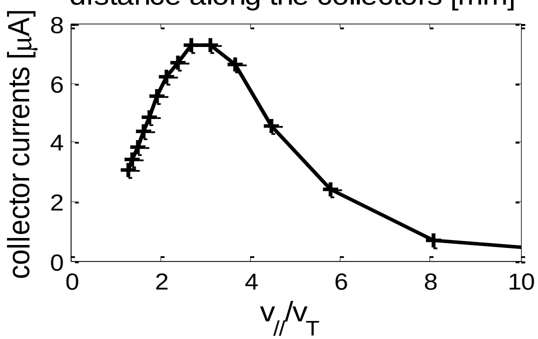

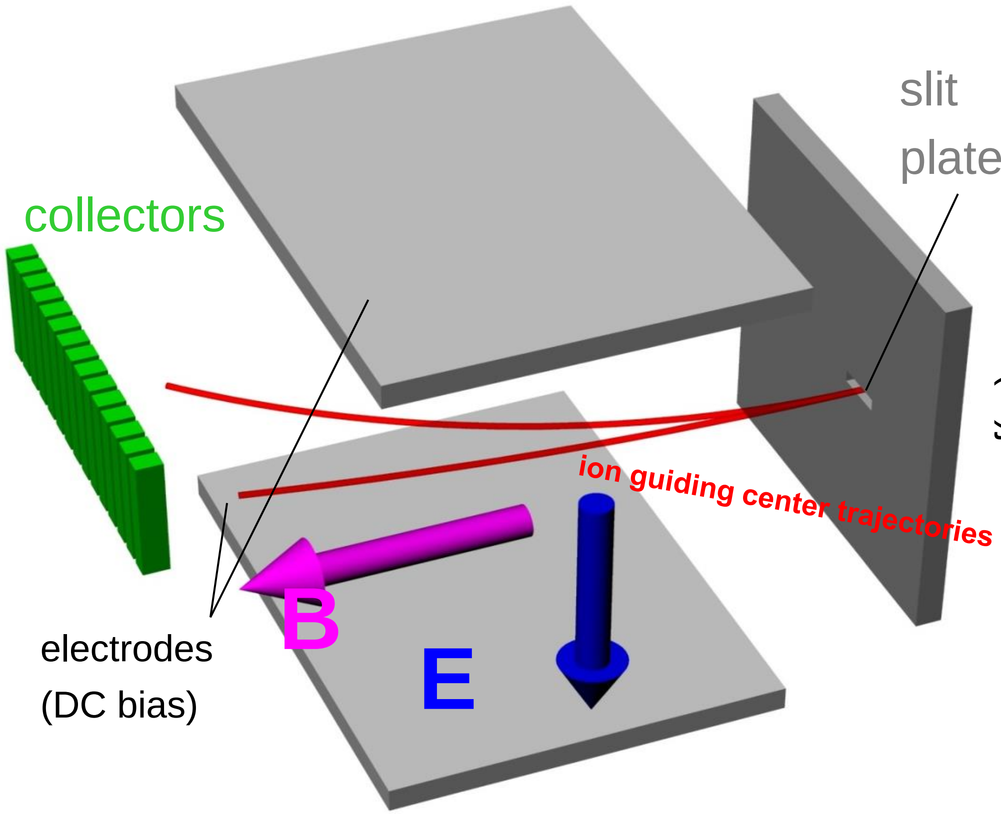

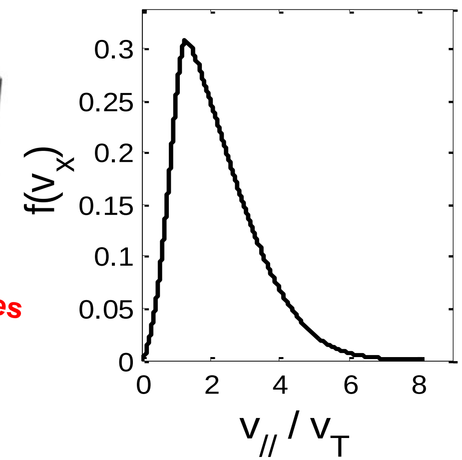

Time resolution determined by DAQ system (2 MHz)

ExB analyzer

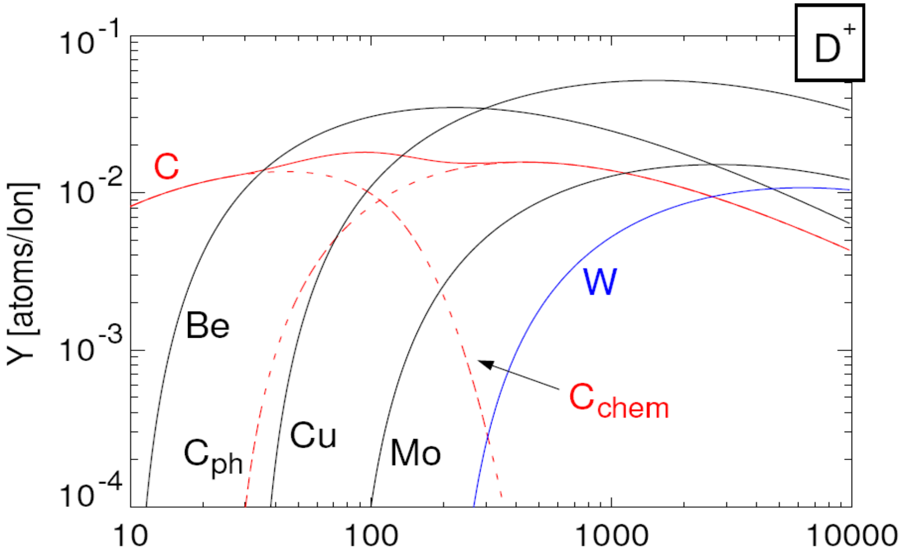

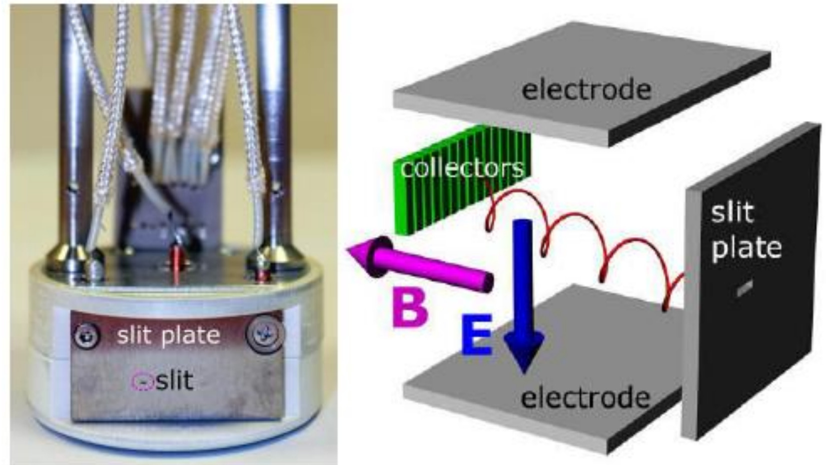

M. Komm, et al., 40th EPS, (2013)

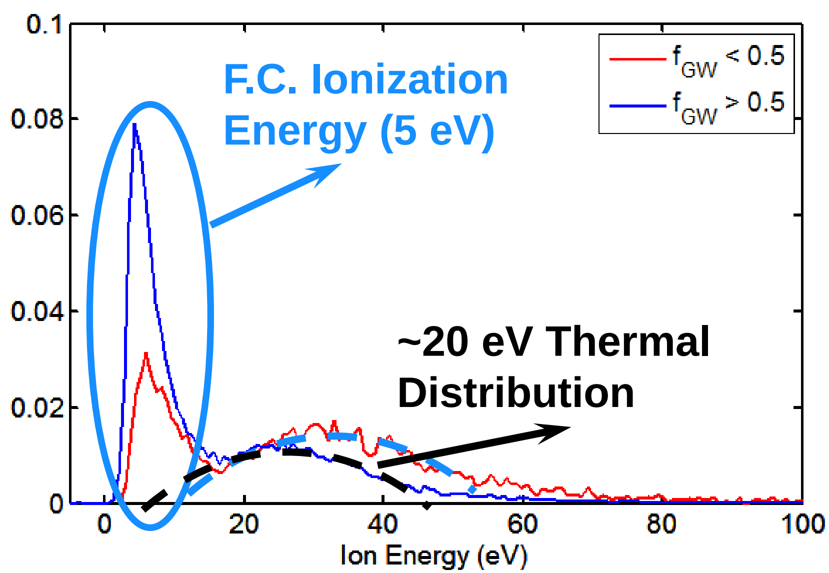

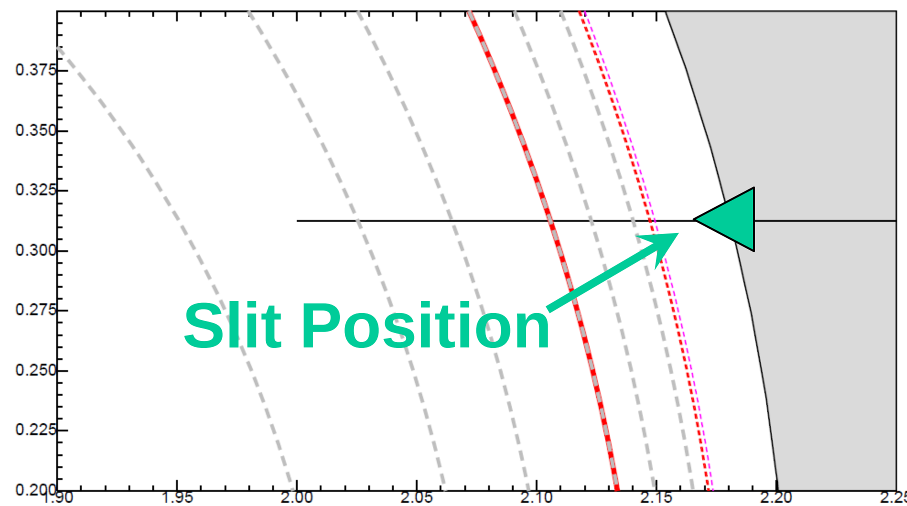

D. Carralero at al., 21st PSI, (2014)

H-mode experiments

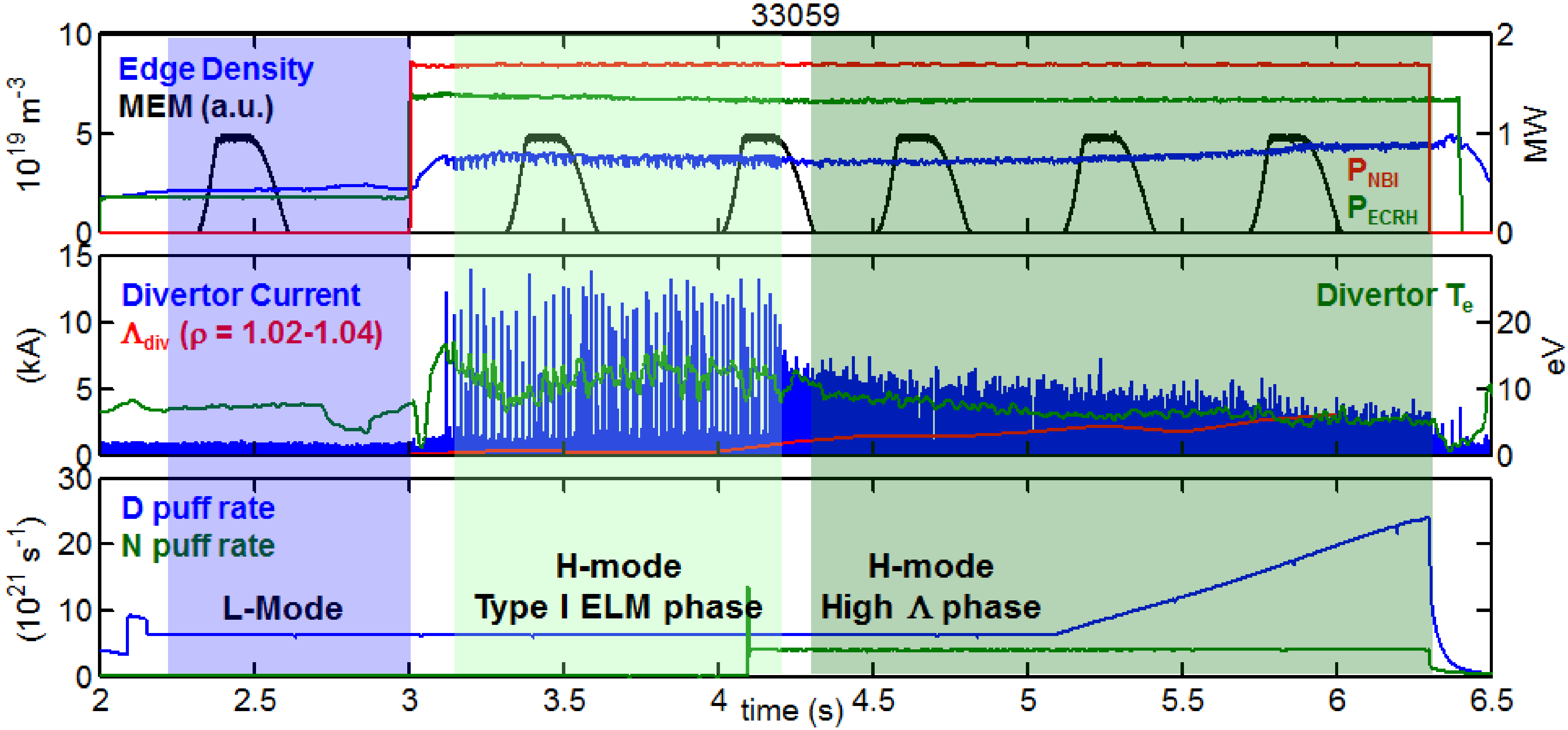

Series of Λ_{div} sweeps with the same magnetic configuration (LSND Edge optimized) and parameters (**B_T = 2.5 T, I_P = 800 kA, q_{95} = 4.85**) as L-mode.

Enough P_{heat} to access H-mode, but avoid damage to the manipulator. $\Lambda_{div} > 1$, is achieved using N seeding and/or large D fueling.

H-mode: Filament transition

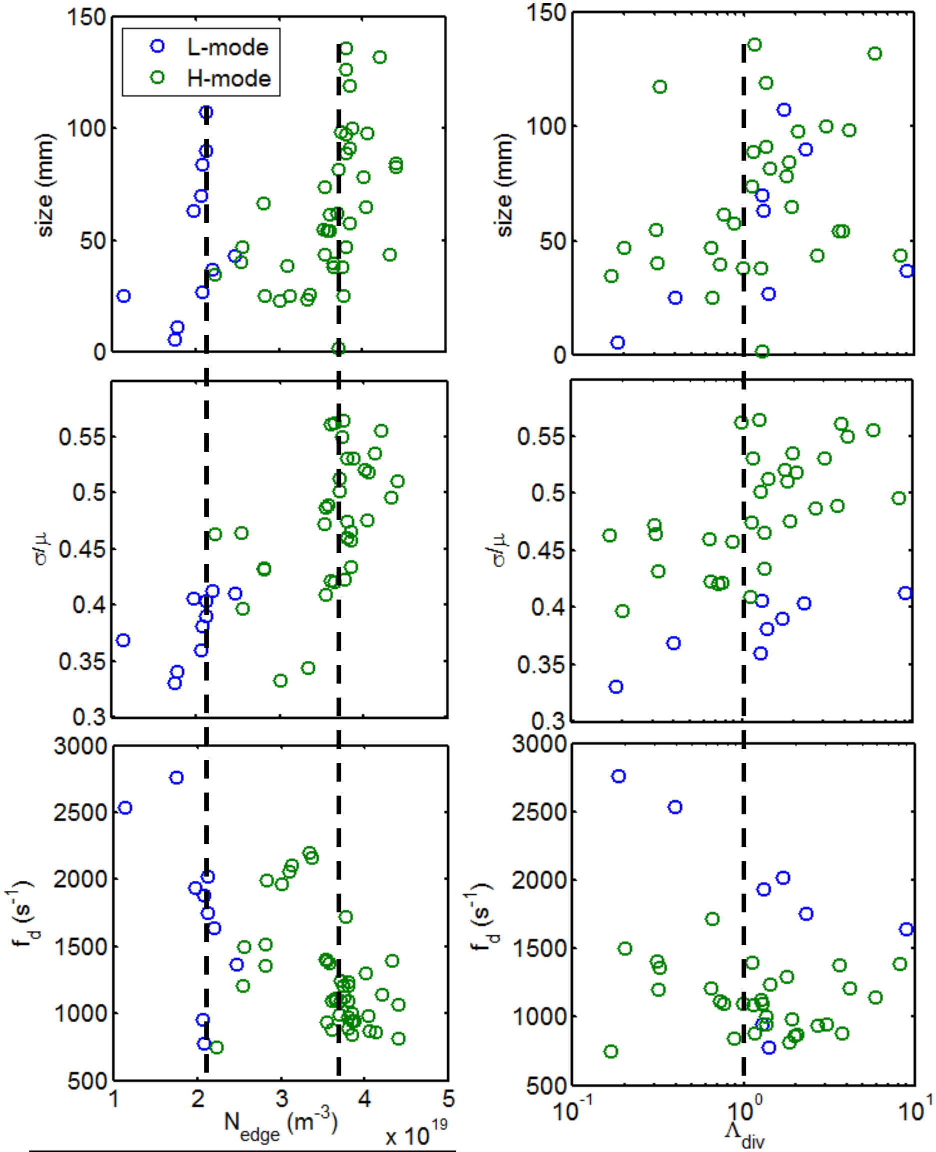

Perpendicular filament **size transitions are observed** for different N_{edge} values at L-mode and H-mode. However, **both happen around Λ_{div} = 1**, in agreement with the SL-IN regime transition model.

Individual discharges show limited data. However, there is **general correlation between δ_b and $\lambda_{n, far}$**.

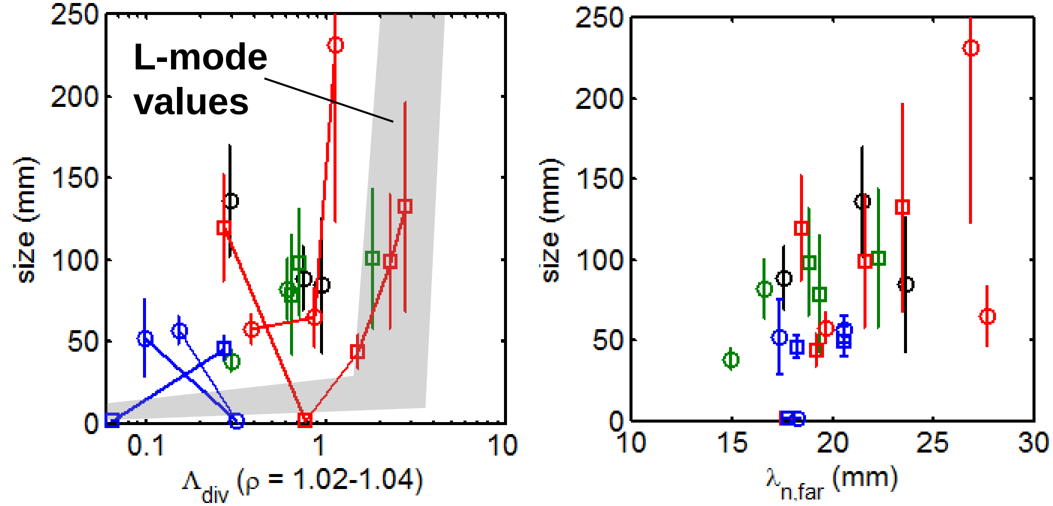

H-mode experiments: Scenarios

Shot	Scenario	P_{ECH} (MW)	P_{NBI} (MW)	$D_{rate\ t=3.5\ s}$ (10^{21} s^{-1})	$N_{rate\ t=4.5\ s}$ (10^{21} s^{-1})	D_{rate} max (10^{21} s^{-1})	N_{rate} max (10^{21} s^{-1})	$T_{e,div}$ min (eV)
31974 (○)	Low N, Low D	1.3	-	1.3	2.8	1.3	3.4	1
31977 (□)		1.9	-	1.3	2.8	1.3	3.8	0
33055 (○)	High N, Low D	1.3	1.7	6	1.8	6	8	1.5
33057 (□)		1.3	1.7	8.2	1.8	8.2	8	3
33056 (○)	High D, no N	1.3	1.7	6.3	-	24.5	-	10
33058 (○)	High D, High N	1.3	1.7	6.3	2	15.4	8	5
33059 (□)		1.3	1.7	6.3	4	24	4	5
33475 (◊)		1.4	1.7	6.2	5	24.4	5	7.5
33478 (Δ)		1.4	2.4	7	9.2	24.4	9.2	1.5

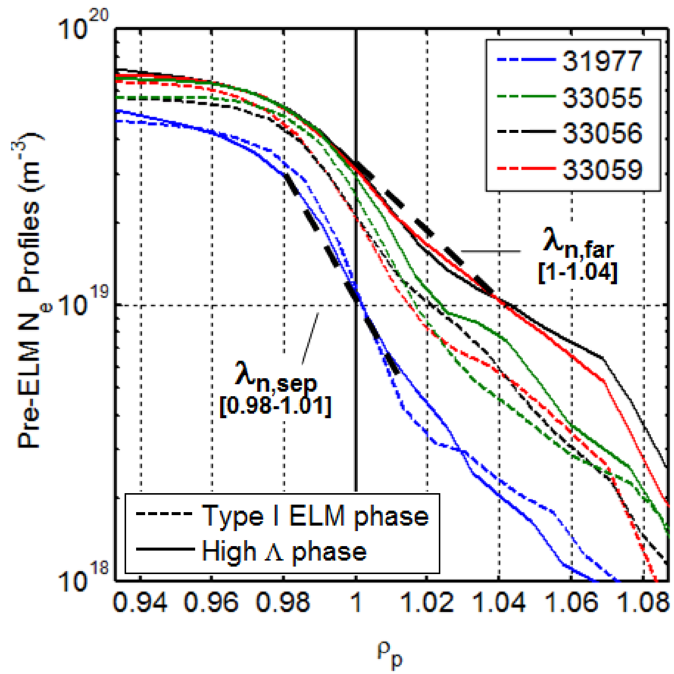

To achieve different levels of Λ_{div}, and disentagle the contributions of D_{rate} and N_{rate}, **4 different scenarios are defined**, based on P_{heat} and the relative amplitude of D fueling and N seeding.

To quantify the degree of shoulder formation, $\lambda_{n,far}$ is defined in the far SOL.

Some scenarios develop a clear shoulder, some others do not.

H-mode experiments: ELM synchronization

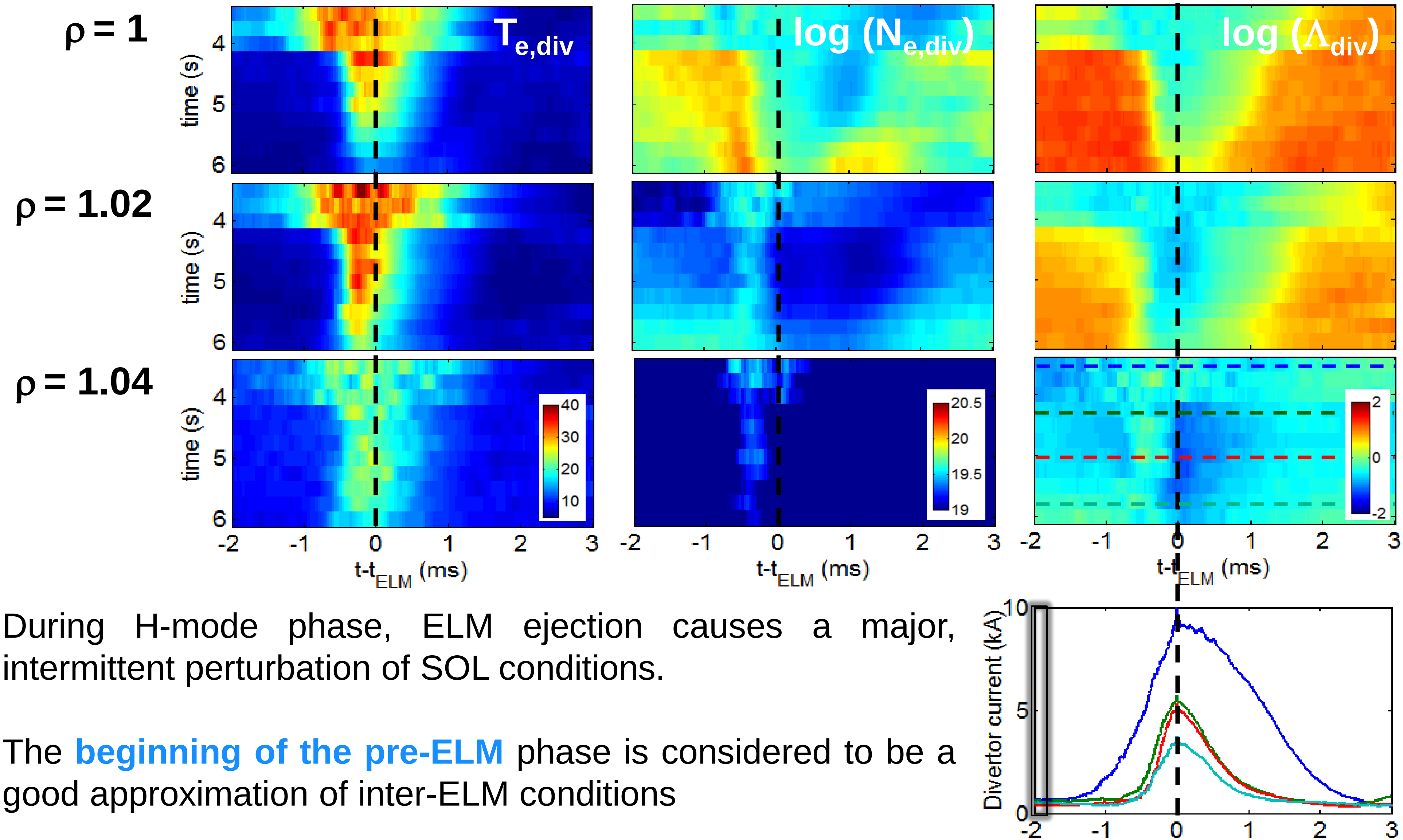

During H-mode phase, ELM ejection causes a major, intermittent perturbation of SOL conditions.

The **beginning of the pre-ELM** phase is considered to be a good approximation of inter-ELM conditions